Transport phenomena in quantum wells and wires in presence of disorder and interactions

Vettchinkina, Valeria

2012

Transport phenomena in quantum wells and wires in presence of disorder and interactions

Valeria Vettchinkina

Division of Mathematical physics
Faculty of Science

Lund University 2012

ISBN-978-91-7473-328-0
Lund-MPh-12/02

Transport phenomena in quantum wells and wires in presence of disorder and interactions

Valeria Vettchinkina

Division of Mathematical physics, LU

Lund University, Sweden

Dissertation for the degree of
Doctor of Philosophy

Thesis Advisor:
Assoc. Prof. Claudio Verdozzi

Faculty Opponent:
Prof. Stefano Sanvito

Academic dissertation which, by due permission of the Faculty of Science at Lund University, will be publicly defended on Tuesday, May 29th, 2012, at 13.30 in lecture hall F, Sölvegatan 14A, Lund, for the degree of Doctor of Philosophy.

Organization
LUND UNIVERSITY
Department of Physics
Division of Mathematical Physics
Box 118, SE-22100 LUND, SWEDEN

Document name
DOCTORAL DISSERTATION
Date of issue
2012-04-23

Author
Valeria Vettchinkina

Sponsoring organization

Title and subtitle
Transport Phenomena in Quantum Wells and Wires in Presence of Disorder and Interactions

Abstract
Present-day electronics employ circuits of smaller and smaller dimensions, and today the length scales are so small that the laws of physics which rule micro-cosmos, quantum mechanics, become directly important. This thesis reports on theoretical work on electron transport in different nanostructures. We have studied semiconductor quantum wells, layered materials where each layer can be only a few atomic layers thick, and transport in thin atomic wires. The layered materials have been studied semi-classically by means the so-called Bolzmann equation and Monte-Carlo techniques. The works on layered materials focused on effects of resonant scattering mechanisms on the electron transport and the feasibility to use semiconductor super-lattices for generating terahertz (THz)radiation. The quantum wires were modeled by 1D Hubbard chains connected to semi-infinite leads and were treated fully quantum-mechanically via the time-dependent density-functional theory (TDDFT). Our TDDFT treatment appears to be able to capture complex features due to competition between correlation and disorder. The merits of the coherent-potential approximation are also analyzed for contacted chains.

In total, four papers are included in the thesis.
In paper I, Monte Carlo simulations of transport in various two-dimensional semiconductor hetero-structures, in particular in cases where accurately calculated scattering probabilities are needed.
In paper II, we present result for electron transport in δ-doped Si/SiGe quantum wells at different temperatures and field strengths.
In paper III, we develop a Monte-Carlo technique to handle electron transport between quantum-well layers when an electric field is applied along the growth direction. We use this method to study scattering-assisted transport under strong fields in the Wannier-Stark regime.
In paper IV, finally, the static and dynamical behavior of 1D Hubbard chains are investigated. The focus is on how the interplay of interactions and disorder affects the localization of fermions in Hubbard chains contacted to semi-infinite leads.

Key words
Lowdimensional semiconducting systems, transport phenomena, disorder, electron correlation, time-dependent density-functional theory

Classification system and/or index terms (if any)

Supplementary bibliographical information

Language
English

ISSN and key title

ISBN-978-91-7473-328-0

Recipient´s notes

Number of pages

Price

Security classification

Distribution by (name and address)

Signature

Date 23 April 2012

List of publications

This thesis is based on the following four articles (which are attached at the end)

I **The Monte Carlo method applied to carrier transport in Si/SiGe quantum wells.**
A. Vettchinkina, A. Blom and M. A. Odnoblyudov
International Journal of Modern Physics B (IJMPB) Volume: 19 No: 21 Year: 2005 pp. 3353-3377

II **Effect of resonant impurity scattering on the carrier dynamics in Si/SiGe quantum wells**
V. A. Vettchinkina, A. Blom, and K. A. Chao
Phys. Rev. B. **96**, 092501 (2005)

III **Scattering-assisted electric current in semiconductor superlattices in the Wannier-Stark regime**
Yu. A. Tarakanov, V. Vettchinkina, M. A. Odnoblyudov, K. A. Chao, N. Sekine, and K. Hirakawa
Phys. Rev. B **72**, 125345 (2005)

IV **Interacting fermions in 1D disordered lattices: Exploring localization and transport properties with lattice density-functional theories**
V. Vettchinkina, A. Kartsev, D. Karlsson and C. Verdozzi
arXiv:1204.0672

Preface

All of our present information technology culture with computers, internet, smartphones, Bluetooth links, 3D-Tv, iPad tablets, programmable washing/cooking machines, car engines, navigation computers, etc. (the list goes on and on) is based on small electrical circuits. The smaller these circuits can be made, the faster and the better microelectronics can perform.

There is much more round the corner: nano-chip technology could soon dim the boundary between living and non-living entities, and perhaps even between us and what is just outside our body: the external world. Some of our capabilities could be improved or fully regained from deficit situations (think of people recovering neural abilities, improving their eyesight, using cyber-prostethics, having real-time monitoring of non-perfect vital functions, etc.)

It is fair to say that some of these developments could impel us to deal with novel bio-ethical conflicts (voices of concern exist already), but science has forced us before to face dilemmas of this sort. Past experience over the last few millennia shows that each time humanity has made a great discovery (e.g. the fire, the wheel, the printing press, the steam engine, the electricity, penicillin, the transistor, internet) the subsequent technological evolution has always proceeded in one direction: forward.

Regaining a more down-to-earth perspective, present-day electrical circuits have reached such small dimensions that the laws of physics which govern the microscopic world, called quantum mechanics, are becoming center-stage. Even within the status-quo of technological development (we refer to it as "nanoelectronics"), it is becoming increasingly important to have a basic understanding of how small systems with a finite number of atoms and electrons behave when subjected to perturbing agents, for example by electric current passing through them.

The knowledge we have of such systems relies, first and foremost, on elaborate and careful experiments. However, experimental data can be difficult to interpret, because even such small systems are in-fact many-particle systems. The analysis can be (and usually is) further complicated by the fact that samples are "disordered", i.e. we have incomplete knowledge and control of the kind of atoms and their positions in the sample.

In principle, theoretical research can contribute significantly to this endeavor, by answering a number of important questions. In practice, often a major obstacle is the lack of accurate theoretical information on how interactions among particles and disorder affect the results.

This thesis is about research work in this direction, namely theoretical investigations of the electric current in different nano-structures. We have analyzed quantum wells (layered slices of semiconductors), and quantum wires (one-dimensional conducting aggregates of atoms). Both are man-made artificial structures where, as their name suggests, quantum effect play an important role in the current trans-

mission. These systems have great potential for technological breakthroughs. We have employed rather different theoretical techniques, aimed to look directly into the behavior of the current in the steady-state (where the current does not change in time), or to follow how the current changes in time to reach such steady state. We have used the Boltzmann's equation, a method with a long and eminent service record in physics, but also a rather new approach (called "density functional theory"), which uses the total electron density as a basic but only variable and therefore requires significantly less computing power than traditional methods.

In the end, the actual common denominator to the different parts of our thesis work is the presence of disorder in our systems. Disorder is ubiquitous in nature: in fact, in many instances, the notion of order corresponds more to our need for simple conceptualizations of reality, than to reality itself (that is, in most cases, in nature, order exists only in an approximate way). Nanoscale systems are no exception and, in fact, the effects of disorder are expected to be strong in these small systems.

From the outside, and especially to the eye of the professional physicist, these considerations can seem a rather tenuous link to thread together somewhat different subjects, systems and methodologies in the same thesis. For us, who worked on these topics for several years, this thesis is a confirmation that, as life itself, scientific research is often made of pieces whose mutual connection is not immediately apparent, and that, in the end, there is beauty in all different parts of Physics.

Acknowledgments

First I would like to say that I consider myself extremely lucky to have met such a large number of great people. I have to start my long list of appreciation with my "home" university, St Petersburg Technical University, Department of Semiconductor Physics and Nanoelectronics. I am happy to say that I felt included in all parts of the department's life, where studies, research and social interaction was equally important. Solid state physics become great fun with help of Anatoliy V. Shturbin, Vadim A. Shalygin, Sergey N. Danilov and my supervisor Dmitriy A. Firsov. My deep appreciation to the symmetry in all its manifestations would not be possible without a course on Quantum Theory of solid states given by Iya P. Ipatova.

To become a PhD student at Lund University turned out to be a life changing experience. I am grateful to my supervisors Koung-An Chao and Irina Yassievich for introducing me to the department and giving me the chance to work with knowledgeable people from all over the world. I would like to explicitly express my gratitude to my coworkers Anders Blom and Yury Tarakanov. Thank you Anders for all your substantial help with all aspects regarding the project. Thank you Yury for being a great collaborator. When the department of Solid State Theory eventually became part of the department of Mathematical Physics, I was introduced to new colleagues that have been very supportive for me, both in my scientific work and my social life.

I am very grateful to my supervisor Claudio Verdozzi for introducing me to the new field of research as well as guiding me trough such a vast area. He has been a very persistent and patient supervisor, and I really appreciate his honesty and sincere interest both in my work progress and well-being as a person.

I also want to thank Carl-Olof Almbladh for his scientific support and advice during my years at the department. And thanks to Alexey Kartsev, for the fun time spent together, when working at one of the projects of this thesis.

I want to thank all my colleagues in the Mathematical Physics department and my special thanks to Katarina Lindqvist and Lennart Österman for making my life much easier and even too comfortable.

My friends were always a very important part in my life. Such a little thing

as changing the country of residence could not affect it. Vera, Ira, Yura, Zhenja, Volodya, Dima and Tolya: thank you guys.

Also my international friends have made me happy, thank you Emilia, Vaida, Natalia, Audrius, Gvidas and Ulrika.

I find it impossible to mention each and everyone here, but nobody is forgotten!

For their immense support, both for my mind and soul I want to thank Daniel Karlsson, Elife Karabulut and Nils Erik Dahlen.

A special part in my "Swedish" life belongs to Lundstedt's family: I want to thank you for making me feel welcome, to make me feel home. Thank you Anna Rubenson, for being such a great source of inspiration during the years! I value very much the opportunity to get to know and to work with Rose-Marie, Anna, Teresia, Rene, Sheela and all the other crew members.

And last, but most important, I want to thank my parents for their encouragement and showing me such dedication no matter what.

Contents

Chapter 1

Non-equilibrium processes in hetero-structures: possibility of THz emission

1.1 Introduction

The generation of far-infrared or terahertz ($1 - 10$ THz; 1 THz$= 10^{12}$ Hz) stimulated emission is of great interest for basic and applied research. From an application point of view, the development of fundamental coherent and tunable THz sources is of great importance in solid state spectroscopy, radio astronomy, medical imaging as well as environmental monitoring. But progress in this area has been hampered by the lack of compact, low-consumption, solid-state terahertz sources. Until recently, available sources of the THz radiation included CO_2 -pumped molecular or Raman gas lasers [1], free electron lasers, backward-wave oscillators. Conventional semiconductor band-gap lasers require sophisticated performance for THz light generation [2]. Another approach for solid state lasers has been realized for intersubband semiconductor lasers. In intra-valenceband p-Ge bulk lasers an upper laser sub-band is populated by electric field heating of heavy holes (lower laser state sub-band) followed by a recombination via an optical phonon. The p-Ge lasers of different modifications cover a broad frequency range (1-4 THz) [3]. However, big energy consumption as well as the low gain of the p-Ge laser restricts their practical use.

The prospect of a semiconductor laser in the infrared and THz region has been one of the key reasons for the development and study of semiconductor hetero-structures. There are a number of physical processes dealing with the THz frequency range specific only for low dimensional semiconductor hetero-structure.

Carrier transitions between sub-bands formed by spatial quantization, interaction with impurity levels, or Bloch oscillations in semiconductor superlattices may give radiation in the THz region. The shift towards hetero-structure lasers were done after realization of quantum cascade laser which is based on a resonant tunneling of the electrons through a system of the specially designed quantum wells. This laser operate on optical transitions between the electron sub-bands. High quantum output have been demonstrated in the broad near- and middle-infrared emission range and continuous wave operation up to the room temperature [4].

Carrier dynamics has been extensively studied in semiconductor hetero-structures with different approaches. One approach relies on self-consistent solution of rate equations of different levels of sophistication [5]. Another uses microscopic, and computationally more demanding, methods based on the Boltzmann equation [6], which employ the Monte Carlo (MC) technique [4, 7]. Rate equation methods rely on the assumption of equilibrium-like carrier distributions over the structure. In contrast, the MC method does not involve any such assumption, and gives a deeper insight into the carrier dynamics.

In the present work we consider two effects that are promising for THz lasering. The first is dealing with creation and repopulation of resonant states induced by impurities. The second is the effect of Bloch oscillations on the conductivity of semiconductor superlattices. These oscillations lead to negative differential conductivity in such systems and consequently to possible gain in the THz region. All simulations of electron transport in quantum wells and superlattices were performed with the Monte Carlo method.

1.2 Hetero-structures

The hetero-layer semiconductor materials with alternating layers of different semiconductors tens of hundreds angstrom thick can be grown by the molecular beam epitaxy or metalorganic chemical vapor decomposition [8]. The change in the forbidden energy gap at the interface leads to the discontinuities in the conduction and valence band edges. These discontinuities form the potential barriers for the electrons and holes so that one degree of freedom is lost (see Fig. 1.1). The carriers can move freely inside the plane of the quantum well but the potential barriers restrict their motion in the transverse direction. A two-dimensional electron gas is formed in the narrow-gap material.

A thin narrow-gap semiconductor together with two layers of wide-gap semiconductors forms a double hetero-junction structure. In the case of low carrier densities the potential profile of such hetero-structure can be approximated by the simple rectangular potential (Fig. 2.2b).

For the electron wave functions and energy spectra the Schrödinger equation is usually solved within the effective mass and the envelope wave function approx-

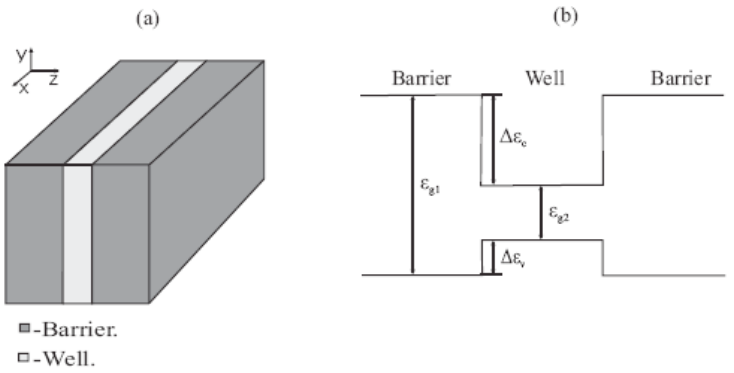

Figure 1.1: Semiconductor hetero-structure (a) and schematic diagram of a double-hetero-junction structure potential profile (b).

imations [9, 10]:

$$\left[-\frac{\hbar^2}{2m^*}\nabla^2 + V(z)\right]\Psi(z) = E\Psi(z). \tag{1.1}$$

where $\hbar$ is the Planck constant, m^* is the electron effective mass and $V(z)$ is the confinement potential. Since the confinement potential acts only in the z direction and electron motion in the (x, y) plane remains free, the one electron wave function can be presented as a product of the partial functions

$$\Psi_\lambda(x, y, z) = e^{i\mathbf{k}\cdot\mathbf{r}}\varphi_\lambda(z), \tag{1.2}$$

where $\mathbf{k}$ and $\mathbf{r}$ are two dimensional wave- and space-vectors, respectively. The total energy of the electron is:

$$E_{\lambda\mathbf{k}} = E_\lambda + \frac{\hbar^2 k^2}{2m_{||}}. \tag{1.3}$$

Inserting Eq. (1.2) into Eq. (1.1) one obtains the equation for the electron envelope function and the energy spectra of the transverse motion:

$$\left[-\frac{\hbar^2}{2}\frac{\partial}{\partial z}\frac{1}{m_\perp(z)}\frac{\partial}{\partial z} + V(z)\right]\varphi_\lambda(z) = E_\lambda\varphi_\lambda(z). \tag{1.4}$$

The eigenvalue E_λ is the bottom of a continuum of levels called a sub-band (see Fig. 1.2). There is a remarkable difference between two-dimensional (2D) and three-dimensional (3D) systems: in a 2D system the density of states is finite even

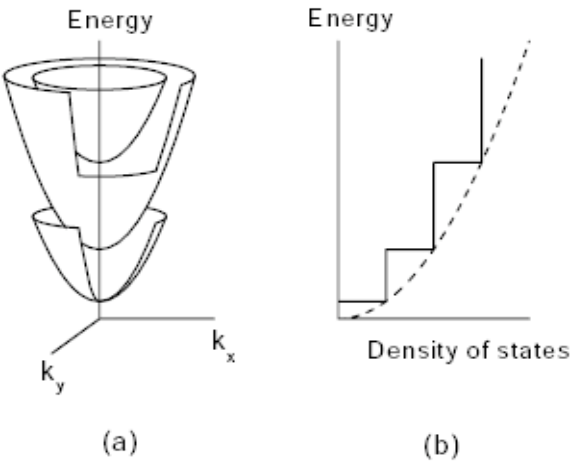

Figure 1.2: Three lowest sub-bands in a quantum well: (a) dependence of electron energy on the in-plane electron wave-vector, and (b) dependence of density of states on electron energy

at the bottom of each sub-band (Fig. 1.2 b) whereas it tends to zero in the 3D case. This has fundamental consequences on the properties of 2D systems as it means that all dynamic phenomena remain finite at low kinetic energies and low temperatures, such as scattering and optical absorption [11].

1.3 Semiconductor superlattices (SSL)

In 1970, Esaki and Tsu suggested that semiconductor superlattice structures can be realized by the periodically repeated deposition of layers from different materials [12]. Since semiconductor superlattices are designed as periodic structures with period d in the growth direction their eigenstates can be chosen as Bloch states $\varphi_\lambda^q(z)$ (where $q \in [-\pi/d, \pi/d]$ denotes the Bloch vector and λ is the band index). The states extend over the whole structure. The corresponding eigenvalues $E(q)$ of the Hamiltonian form the band. This provides the exact solution for a perfect superlattice without applied electric field. Both the energy width Δ of these bands, as well as the extension $2\pi/d$ of the Brillouin zone, are much smaller than the corresponding values for conventional conduction bands. Thus, the energy bands originating from the superlattice structure are called minibands.

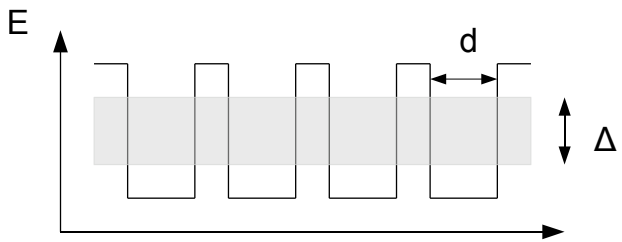

Figure 1.3: Sketch of conduction band of semiconductor superlattice with miniband in equilibrium

An alternative set of basis functions can be constructed by employing localized wave functions which resemble eigenstates of single quantum wells labeled by the index n. The Wannier-states $\Phi_\lambda(z - nd)$ can be constructed separately for each miniband index:

$$\Phi_\lambda(z - nd) = \sqrt{\frac{d}{2\pi}} \int_{-\pi/d}^{\pi/d} dq e^{-inqd} \phi_q^\lambda(z) \tag{1.5}$$

Both of these approaches are equivalent, but the second approach is more appropriate for investigations of carrier dynamics in SSL in case of high electric field applied along superlattice structure.

In the 2D systems one degree of freedom of the carriers is restricted by the confinement potential associated with an interfaces leading to quantization of the momentum in that direction, while motion in the remaining two directions is unconstrained. Hence the question of great importance is direction of applied external electric field. In case of transport parallel to confining potential we can discuss the transport properties of such system in terms of macroscopic parameters such as conductivity, drift velocity and so on within semiclassical approach. Transport perpendicular to confining barriers we will consider in case of SSLs where semiclassical approach valid only within small range of applied external electric fields while one can justify existence of miniband. In order to investigate transport in SSL with such a direction of applied field we will employ Wannier approach to superlattices.

If an electric field $\mathbf{F}$ is applied, the Bloch states are no longer eigenstates of the Hamiltonian. In the conventional semiclassical approach the Bloch vector $\mathbf{k}$ becomes time dependent. In 1928 Bloch [13] showed that a wave packet given by a superposition of single band states peaked about some quasi-momentum, $\hbar\mathbf{k}$, moves with a group velocity given by the gradient of the energy-band function with respect to the quasi-momentum and that the rate of change of the quasi-momentum is proportional to the applied field $\mathbf{F}$ what is known as acceleration

theorem:

$$\hbar\dot{\mathbf{k}} = \mathbf{eF}. \tag{1.6}$$

In case of static electric field that is applied along quantum well (QW) layer electron dynamics can be represented by a uniform drift of the carriers in k-space along the field direction since wave function corresponds to free electron motion in that direction [11].

In case of the field applied along the z axis parallel to the growth direction, in the effective mass approximation the wave functions in the xy plane are still simply plane waves with the corresponding eigenenergies $\varepsilon_{\mathbf{k}_{||}} = \hbar^2(k_x^2 + k_y^2)/(2m)$. As we pointed out earlier the total wave function $\Psi_{\lambda\mathbf{k}_{||}}(r)$ can be expressed as

$$\Psi_{\lambda\mathbf{k}_{||}}(\mathbf{r}) = \frac{1}{\sqrt{S}} \exp(i(k_x x + k_y y))\psi_\lambda(z), \tag{1.7}$$

where S is the normalization area. The wave function $\psi(z)$ and the corresponding eigenenergy E_z , which describe the energy spectrum in this case, must be derived from the Schrödinger equation

$$\left[-\frac{\hbar^2}{2}\frac{\partial}{\partial z}\frac{1}{m_\perp(z)}\frac{\partial}{\partial z} + V(z) + eFz\right]\psi(z) = E_z\psi(z). \tag{1.8}$$

Wannier [14] pointed out that due to the translational symmetry of the crystal if function $\psi(r)$ is an eigenfunction of the scalar potential Hamiltonian (corresponding to the perfect crystal plus external field) with eigenvalues ε than any $\psi(r + nd)$ is also eigenfunction with eigenvalue $\varepsilon + n\Delta\varepsilon$, where $n\Delta\varepsilon = eFd$ is so called Wannier-Stark splitting (d being the primitive lattice vector along the field direction). He concluded that the translation symmetry of the crystal gives rise to discrete energy spectrum - Wannier Stark Ladder (WSL). Since the samples used in experiments are of finite length, the potential function $V(z)$ in the above equation should be a multiple-period square-well potential, bounded at each end by a higher potential barrier simulating the work function. We will solve Eq. (1.8) by expanding $\psi(z)$ in terms of a complete set of basis functions. The Bloch states of each miniband in this SSL can be derived easily. Since the Zener tunneling (between two energy minibands) will not appear in the system to be studied here, we will treat individual sub-bands separately and for the convenience we will skip the band index since we will work within one lowest miniband. From the Bloch states of a given miniband, we can construct the complete set of Wannier functions $\Phi(z - nd)$, where n runs over all integers. To avoid any ambiguity in our future description, we will enumerate our eigensolutions according to their spatial location, and use the terminology that the eigenstate $\psi_i(z)$ is localized in the ith unit cell of the SSL sample. Then, we expresses the wave function $\psi_i(z)$ as

$$\psi_i(z) = \sum_n f_n^i a(z - nd), \tag{1.9}$$

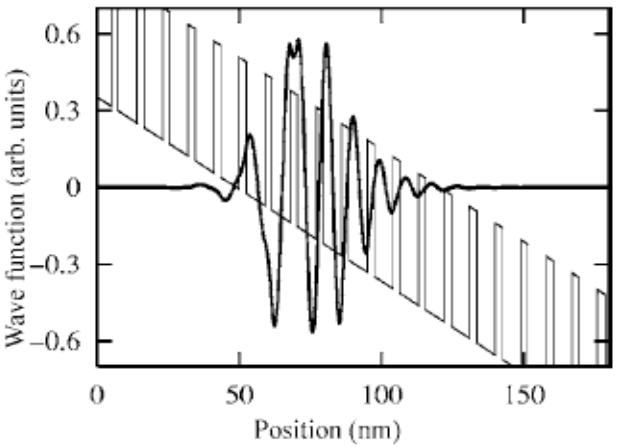

Figure 1.4: Example of the wave function corresponding to a Wannier-Stark level under an electric field. The thin line indicates the conduction band edge profile (Paper III)

were a is a Wannier basis function and where f_n^i is an expansion coefficient. The coefficients $\{f_n^i\}$ and corresponding energy eigenvalues $\{E_z^i\}$ for a SSL sample of finite size can be obtained by diagonalizing the field-dependent Hamiltonian matrix

$$H_{i,n}(F) = \int_{SL} dz\, a^*(z - id)H(F, z)a(z - nd). \tag{1.10}$$

For further details the reader is referred to Ref. [15]. Eigenfunctions $\psi_i(z)$ in the WSL are spatially equally separated by the lattice constant d , in agreement with the theoretical predication of Wannier [16]. The total energy of the electron in the SSL is then

$$E^i_{\mathbf{k}_{||}}(z) = E_z^i + \varepsilon_{k_{||}} \tag{1.11}$$

The states corresponding to these equidistantly spaced levels are localized states, as schematically shown in Fig. 1.4 for the case of semiconductor superlattice. The degree of this WS localization depends on the strength of applied field.

1.4 Boltzmann transport equation

Conventionally, kinetics in semiconductor hetero-structures is treated semi-classically via the Boltzmann transport equation [18]. The Boltzmann equation may be de-

rived by writing continuity equation in the 2n-dimensional phase space in terms of the particle flux through a small volume of this space around **r** and **k** [19]

$$\frac{\partial}{\partial t} f_i = -\frac{1}{\hbar} \nabla_{\mathbf{k}} \mathcal{E}(\mathbf{k}) \cdot \nabla_{\mathbf{r}} f_i - \frac{e}{\hbar} \mathbf{F} \cdot \nabla_{\mathbf{k}} f_i + \left| \frac{\delta f_i}{\delta t} \right|_{collision}, \tag{1.12}$$

where $\mathcal{E}(\mathbf{k})$ is the energy associated with state **k**, and **F** is electric field. The last term in Eq. (1.12) represents the rate of change due to scattering and may be written as balance of in- scattering and out scattering events as collision integral,

$$\left| \frac{\delta f_i}{\delta t} \right|_{collision} = \sum_{j,\mathbf{k}'} S_{j,i}(\mathbf{k}, \mathbf{k}')[f_j(\mathbf{k}')(1 - f_i(\mathbf{k}))] - S_{i,j}(\mathbf{k}, \mathbf{k}')[f_i(\mathbf{k}')(1 - f_j(\mathbf{k}))]. \tag{1.13}$$

Here, $S_{j,i}(\mathbf{k}, \mathbf{k}')$ represents the scattering rate from a state in sub-band j of wave-vector **k** to a state in sub-band i with wave-vector $\mathbf{k}'$. The collision integrals of the Boltzmann equation are the functions of the scattering rates, and the electron wave functions are required for the scattering rate calculation. Once the distribution function is known, all quantities of interest, such as carrier drift velocity and mean energy can be obtained as functions of the applied field and temperature. It is quite hard to obtain solutions to the Boltzmann equation by analytic means. Even in the linear response case, with simple scattering mechanisms, approximations are needed. In most cases one has to introduce crude approximations and simplifications in order to obtain closed-form analytic solutions for systems of interest. One might say that simplified analytic solutions to the Boltzmann equation provide general insight into linear and non-linear transport phenomena but that they lack predictive power. An important step forward in the solution of the Boltzmann equation has been achieved by introducing numerical techniques. The Monte Carlo method is by far the most popular numerical technique [7, 20]. The application of Monte Carlo techniques to high-field transport in semiconductors was introduced by Kurosawa at Semiconductor Conference held in Kyoto in 1966 [21]. Since then the method has been greatly improved and widely used to obtain results for various situations in practically all materials of interest. Among the most significant developments of the Monte Carlo technique are the work of Price [22], of the Malvern group [23, 24, 25, 26, 27] with the introduction of the self-scattering scheme and the extension of the method to many-particle simulations [28], to harmonic fields [22] and to degenerate statistics [29, 30]. The Monte Carlo solution of the Boltzmann transport equation not only gives the distribution function that verifies the equation, but also yields information on its fluctuations that is lost in the Boltzmann equation itself [31].

1.5 Mechanisms of THz emission in 2D semiconductor hetero-structures

Semiconductor hetero-structures have been the subject of intensive studies due to their great flexibility as model systems for research as well as for industrial implementations. For example by varying composition of semiconductor during the growth procedure one can construct hetero-structure with desirable band gap profile (including energy distance between sub-bands) or by varying external electric field change the corresponding position of energy levels (energy distance between Wannier-Stark levels). Understanding and prediction of the the carrier dynamics in systems with such complicated structure is an important issue for the design of structures where conditions for THz lazering are fulfilled.

In this work we will consider two mechanisms that lead to THz radiation in hetero-structures with 2D electron gas under external applied electric field. With electric field applied along hetero-structure layers we are going to investigate resonance scattering channel and effect of it to distribution function. In case of superlattices we are interested in dynamics in direction of spatial quantization (along miniband) and resulting region with negative differential conductivity caused by Bloch oscillation (BO) of carriers under applied dc electric field.

1.5.1 Resonant states induced by impurities

Resonant states of so-called Fano type, i.e., a discrete, and hence localized state, degenerate with a continuum, are well known from atomic physics [32], bulk semiconductors [33, 34, 35, 36, 37] and quantum wells [38, 39, 40, 41]. We will consider resonant states induced by impurities and placed in semiconductor hetero-structures.

Impurity states in hetero-structures have been the subject of detailed investigations during the last three decades. Traditionally, impurities are considered as a purely negative factor for carrier dynamics, since their presence are increasing the scattering rates. On the other hand, doping is essential to supply enough free carriers into the system. The general trend has therefore been to remove the doping region from the active region by using modulation doping. Recently, however, impurities have been placed in the active region of Si/SiGe quantum well structures with idea to apply their properties for novel optical devices in the far-infrared or terahertz region [42, 43, 44]. Si and Ge are non-polar materials with low intrinsic absorption at THz frequencies. Taking into account also the possibilities for integration with existing device technology [45], these systems appear very attractive for optical applications in the THz region, which recently has received a lot of attention in a variety of fields [46]. A detailed knowledge of the properties of impurity states in Si/SiGe hetero-structures and their effect on carrier distribution is therefore essential.

The system of interest here is lattice mismatched $Si/Si_{1-x}Ge_x/Si$ quantum wells with delta doping. The combined effect of confinement and internal strain results in the splitting of the acceptor levels and formation of acceptor resonant states, similar to those in strained p-Ge. These points, together with the possibility of monolithic integration of silicon-based electronic and optoelectronic components, are strong incentives for the development of a SiGe quantum cascade laser.

In narrow quantum wells, the lowest antisymmetric impurity state, which is bound to the second QW sub-band, may become resonant with the continuum of the first sub-band [47, 48], - i.e. if symmetry allows it, the localized state can couple or hybridize with the continuous states. The resonant state is then characterized by an energy width, which is immediately related to its lifetime [32]. When the impurity is placed outside the well, in the barrier, similar but entirely different resonant states may also be formed from the usual shallow donor levels, and their widths can be evaluated by the resonant coupling method [49]. Attempts have been made to apply an essentially equivalent method for the case of donors inside the well [50, 51, 52]. It has however been shown that the approximations made in this approach are rather severe [53].

It is possible to populate a coupled resonant state by heating carriers with parallel to QW dc electric field from the bottom of the sub-band, until they reach the resonance energy [37, 54]. They may then be captured into the resonant state, and possibly make an optical transition to the ground state. If an inverted population could be arranged between the resonant state and the ground state, one could realize a laser based on this process. A particularly appealing point of such a device is that since the impurity states are attached to the QW levels, it is possible to control the intra-impurity transition energy by varying the QW parameters. Experimental evidence of optical transitions involving coupled resonant states in quantum wells exists from both Raman scattering [55] and absorption spectroscopy [56] measurements.

1.5.2 Bloch oscillations

In an ideal SSL or crystalline material (without scattering) subject to an electric field $\mathbf{F}$, the quasi-momentum $\hbar\mathbf{k}$ of an electron will move with constant speed in $\mathbf{k}$ space when viewed in an extended zone scheme, $\hbar\dot{\mathbf{k}} = e\mathbf{F}$. Because the energy $\epsilon_{\mathbf{k}\lambda}$ and thereby the group velocity is a smooth periodic function of $\mathbf{k}$, the electrons would execute a periodic motion in real space with a Bloch-oscillation (BO) frequency $\hbar\omega_B = edF$. When reduced to the first Brillouin zone, $\mathbf{k}$ would undergo a Bragg reflection when it hits a zone boundary, which leads to a discontinuous periodic motion in $\mathbf{k}$ space and the same continuous periodic motion in real space. As is well known scattering completely change this behavior in normal crystalline materials. An electron can then only complete a small fraction of a BO period before it is scattered into another state, and the scattering mechanisms then lead

to normal ohmic conduction.

In a man-made SSL, the Bloch period is much smaller owing to the smaller Brillouin zone, and following the proposal of Esaki and Tsu [12], the possibility of Bloch oscillations in SSL has attracted great interest. In particular, Bloch oscillation in semiconductor superlattices is attractive as a source of coherent terahertz electromagnetic waves, because the frequency of the radiation can be tuned in the THz range by dc bias fields. Since the first proposal of high-frequency Bloch oscillators by Esaki and Tsu, considerable effort from both experiments [57, 58, 59, 60, 61, 62, 63, 64] and theories [65, 66, 67, 68, 69] has been made to search for Bloch oscillations and obtain THz emission. Ultra-fast time-domain experiments demonstrate that electrons in SL minibands perform at least a few cycle BOs [58, 61, 62, 70, 71]. However, the idea of the Bloch oscillator was challenged by asking whether BO is useful in generating (amplifying) electromagnetic waves [72]. In the Wannier approach to miniband transport, the emission and absorption of EM waves take place between the adjacent two WS levels; hence they occur at the same frequency and cancel each other. Consequently, an ideal SL has no net gain or loss for electro-magnetic waves. However, when scattering exists in the system, new transition channels, i.e., scattering-assisted transitions, become available [73]. Scattering processes cause transitions between Wannier-Stark states which are the eigenstates of the superlattice in an electric field yielding a THz emission with Bloch frequency and a net current in the direction of the electric field [74]. Esaki and Tsu [12] pointed out that in such a system the electrons can demonstrate a negative differential drift velocity with increasing field what gives rise to a gain in the frequencies of the order of the Bloch frequency. It was suggested that Bloch oscillations responsible for it. Only now the availability of high-quality semiconductor superlattices with controllable lattice periodicity has stimulated extensive investigation on phenomena relevant to the possibility of THz gain. Therefore, it is very crucial to clarify the nature of the scattering mechanisms in superlattices.

Chapter 2

The Monte Carlo Technique with application to Boltzmann transport

The most commonly used approach for the theoretical analysis of energy relaxation as well as transport experiments is the Monte Carlo (MC) method [7], both in bulk and in low-dimensional structures. One can describe Monte Carlo method as simulated experiment which possesses a great flexibility. This has proved to be a very powerful technique allowing the inclusion at a kinetic level of a large variety of scattering processes. Indeed, the extremely predictive character of the MC simulation strategy in the design and optimization of current optoelectronic devices has been recently confirmed by fully three-dimensional simulations of transport as well as lasing properties of light sources both in the mid- and far-infrared spectral regions [4].

Monte Carlo methods are the numerical methods based on the random quantities. As applied to the electron transport in the semiconductor systems, the Monte Carlo method consists of a simulation of one or several electron motion inside the crystal. The electrons move in the external electric and magnetic fields. The motion of the electrons is interrupted by the scattering events. The duration of electron free flight between two successive collisions and the scattering mechanism responsible for the end of the free flight are selected stochastically in accordance with scattering probabilities describing the microscopic process [31]. Monte Carlo model relies on generation of sequences of random numbers with given distribution probabilities. Monte Carlo technique became popular with the advent of computers, as computers can generate sequences of random numbers evenly distributed between 0 and 1 at sufficiently fast rate. Random numbers x with a given probability distribution $f(x)$ in an interval (a, b) can be generated starting from random

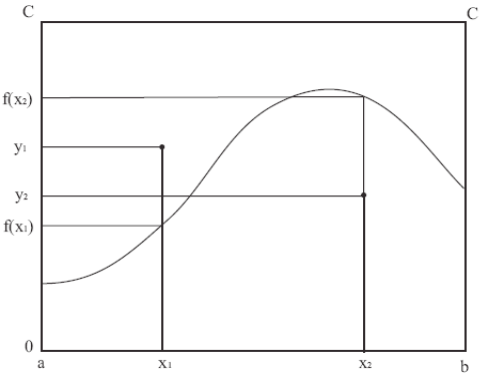

Figure 2.1: Rejection technique for the random number x with distribution f(x) generation starting from evenly distributed random numbers.

number r evenly distributed in the interval $(0, 1)$. The simplest way is to solve integral equation:

$$r \int_a^b f(x)dx = \int_a^x f(u)du \tag{2.1}$$

Sometimes, the above simple technique cannot be applied, because it is not possible to evaluate analytically the integrals or to solve the equation with respect to x. In these cases rejection technique can be used.

With the rejection technique, the pairs (x, y) of random numbers are generated, where x is the random number with flat distribution in (a, b) and y in $(0, C), C$ is positive number such that $C \geq f(x)$ in the whole interval (a, b) (Fig. 2.1). If

$$y \leq f(x_1) \tag{2.2}$$

then x_1 is retained as choice of x, otherwise x_1 is rejected, and a new pair is generated until equation 2.2 is satisfied. The probability of accepting x_i is proportional to $f(x_i)$, as desired. When steady state homogeneous phenomenon is under investigation, it is sufficient to simulate the transport of one electron. From the ergodicity we can assume that the electron motion simulation for the sufficiently long time will give information about behavior of the entire electron gas. However, if the transport process is not homogeneous or is not stationary (time dependent electric or magnetic fields, inhomogeneous systems), we cannot rely on the ergodicity of the system, and it is necessary to simulate the ensemble of electrons. In

our calculations we will use the Ensemble Monte Carlo, as it is more general. Figure 2.2 shows the structure of the typical Monte Carlo program for the electron transport simulation in a semiconductor. The simulation starts from the definition of the physical system: the hetero-structure, the parameters of the materials, the energy dispersion relations, and the values of physical quantities, such as electric field strength and lattice temperature. Some parameters, such as coupling strengths for alloy disorder and acoustic scattering, hot phonon relaxation times when they are not well known, can be used as fitting parameters. At this step the parameters that control the simulation should be defined. Such parameters are duration of electron transport, number of electrons simulated, precision of electron distribution function and so on. When the physical system is defined, the next step is generation of the initial conditions for each electron under simulation. In the case of electron transport in a homogeneous material, only wave vector for each electron should be defined. If the steady-state situation is simulated, the simulation time should be long enough to avoid the influence of initial conditions.

When a highly inappropriate initial conditions are generated, the initial part of the simulation can be influenced by this inadequate choice. The time of simulation must be long enough to exclude influence of the initial conditions on the electron transport. In order to avoid the undesirable effect of an inappropriate initial conditions on average results and to obtain better convergence, we eliminate the first part of the simulation from the statistics. When we are dealing with low electric field electron transport, we use equilibrium Fermi-Dirac or Boltzmann distribution functions to generate initial electron velocities. However, if a very high electric field is applied, the electron energy generated by the equilibrium distribution is much lower than the average energy in the steady state conditions, and a big part of initial transient should be excluded from the statistics. As electron is moving in the applied electric field $\mathbf{F}$, its wave vector $\mathbf{k}$ changes continuously according to the acceleration theorem 1.6. In order to find electron wave vector just before scattering event, one should know electron free flight time. The probability $P(t)$, that electron will suffer its next collision during dt around t is given by:

$$P(t)dt = W[\mathbf{k}(t)]exp\left[-\int_0^t W[\mathbf{k}(t')]dt'\right]dt \tag{2.3}$$

The integral at the exponent usually is complicated and rejection technique should be used to generate electron free flight according to 2.3. As electron free flight time should be generated after each scattering event, the use of the rejection technique would dramatically increase simulation time. Rees [23] has devised a simple method to overcome this difficulty. A new fictitious 'self-scattering' is introduced, such that the total scattering probability (the sum of all real scattering probabilities plus self-scattering) is constant and equal to $\Gamma \equiv t_0^{-1}$. If the carrier undergoes a self-scattering, its state after scattering event $\mathbf{k}'$ is taken to be equal to its state

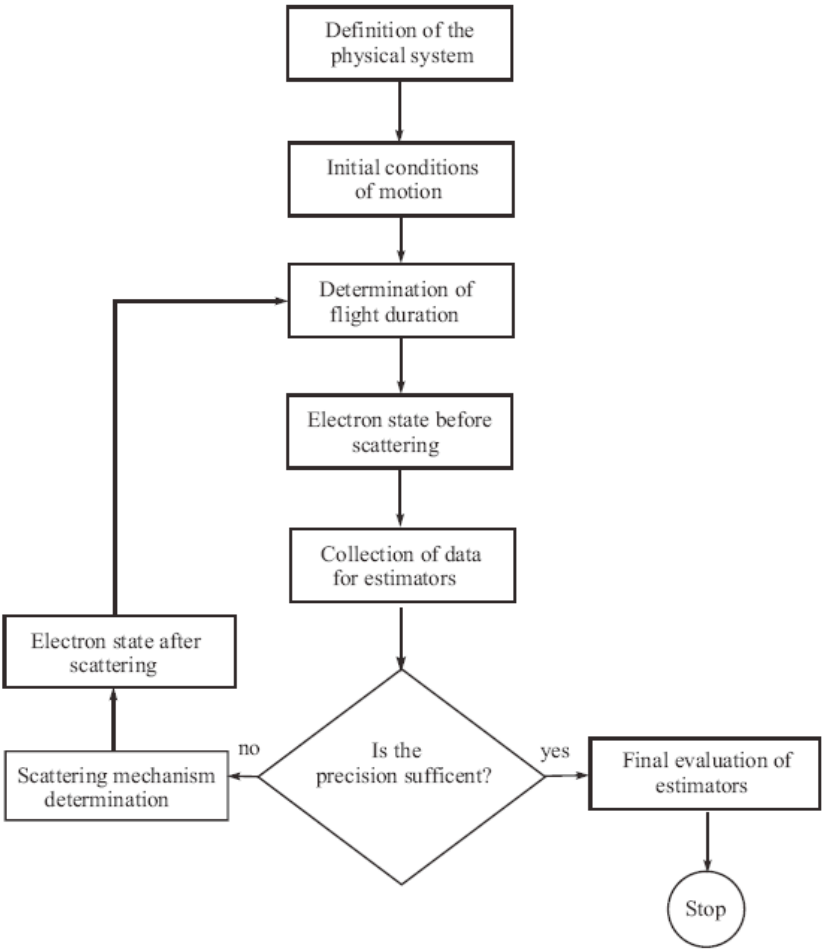

Figure 2.2: Flowchart of a typical Monte Carlo program [7].

before scattering event, so that in practice the electron path continues unperturbed as if no scattering at all have occurred. The value of G is the maximum value of $P(\mathbf{k})$ in the region of $\mathbf{k}$ space in interest. Now, with a constant $P(k) = t_0^{-1}$, equation 2.3 reduces to:

$$P(t) = \frac{1}{\tau_0} exp(-t/\tau_0) \tag{2.4}$$

and random evenly distributed numbers r can be used to generate stochastic electron free flights t_{tr} using Eq.(2.1):

$$t_{tr} = -\tau_0 ln(1-r) \tag{2.5}$$

Using the technique proposed by Rees, simulation time is increased, as one has to take care of self-scattering events. However this increase is in general, more than compensated for by the simplification in calculating the free-flight duration. During the free flight, electrons are moving according to acceleration theorem. At its end the electron wave vector $\mathbf{k}$ is known, and all scattering rates $W_j(\mathbf{k})$ can be evaluated, where j indicates the number of the scattering mechanism. The probability of self-scattering will be a complement to Γ of the sum of the all real scattering mechanisms. The scattering mechanism responsible for the end of the free flight must now be chosen among all those possible, according to the relative strength of all scattering mechanisms. The evenly distributed random number r is generated and the product $y = r\Gamma$ is compared with the successive sums of the $W_j(\mathbf{k})$. The jth scattering mechanism is chosen if j is such that the first of the partial sums $W_1, W_1 + W_2, W_1 + W_2 + W_3, ...$ is larger than y:

$$y < W_1 + W_2 + \cdots + W_j \tag{2.6}$$

The Monte Carlo approach for solving the Boltzmann transport equation is naturally valid under the same conditions as Boltzmann equation itself. This means that all scattering events are assumed to occur instantaneously.

Once the scattering mechanism responsible for the end of the electron free flight has been determined, the new electron state after scattering must be chosen as the initial state for the next electron free flight. When a true scattering has occurred, the electron state after scattering must be generated stochastically, according to the differential cross-section of the scattering mechanism $W_{if}(k, k')$ responsible for the end of the free flight. Since electron scattering differential cross-sections for the 2DEG are complicated, we employ rejection technique to find electron state after scattering. In the Ensemble Monte Carlo, the motion of all electrons is performed as described earlier. The history of each electron is subdivided into equal time intervals and all required data is collected at the end of each interval. The average value of quantity $\langle A(t) \rangle$ is defined as the ensemble average at time t over N electrons of the system:

$$\langle A(t) \rangle = \frac{1}{N} \sum_i A_i(t) \tag{2.7}$$

The electron mean energy and drift velocity can be calculated, after Eq. (2.8). For calculation of the electron distribution function, two-dimensional electron wave vector $\mathbf{k}$-plane is subdivided into cells of fixed area Δk, and the number of simulated electrons in each cell is calculated. The steady-state electron distribution

function is proportional to the number of electrons $n(\mathbf{k})\Delta k$ that at time t are found to be in a cell $\Delta\mathbf{k}$ around $\mathbf{k}$. Energy relaxation time may be computed from the Monte Carlo simulation in following way. Electron energy relaxation time is estimated from the power gain-loss balance:

$$\tau_\xi(E) = \frac{\xi(E) - \xi(0)}{V_{dr}(E)E} \tag{2.8}$$

where $\xi(E)$ is the electron mean energy, $V_{dr}(E)$ is the electron drift velocity and E is the strength of the applied electric field. Electron mean energy and drift velocity can be evaluated from the Monte Carlo simulation. Supposing that the electron energy relaxation usually is non-exponential, only effective energy relaxation time can be calculated from the energy balance equation.

Two types of hetero-structures were involved in our investigation. First is single QW structure, where we consider effect of resonant scattering on drift velocity and populating of resonant state. Second is multiple QW structure - superlattice with idea of investigating effect of Bloch oscillations on drift velocity in a regime with negative deferential conductivity. In both cases 2D distribution function (in a layer of QW) were simulated. In case of single QW external electric field were applied along QW layer what causes electron heating and repopulating of different valleys and sub-bands – within MC approach we treated distribution function in two sub-bands – general MC. In case of superlattice, fields were applied perpendicular to QW layers. Field were too high to consider system within semiclassical approximation. As mentioned earlier the energy spectrum of a Bloch electron under an external dc field $\mathbf{F}$ consists of an infinite series of eigenvalues which are equally separated by an energy difference eFd but with usual quadratic dispersion in quantum well layer. Current in a field direction then was caused by a carrier hopping between Wannier-Stark states due to different scattering mechanisms. Within MC simulation both 2D distribution function within quantum well layer and transitions between Wannier-Stark states were taken into account. Information about number of transitions along the field direction and against gave the value of the current trough the system. For details of Monte Carlo calculations specific to each case, see Chapter[3] and Chapter[4].

Chapter 3

Electron transport in the presence of resonant scattering in Si/SiGe hetero-structures

The formation of resonant states is accompanied by the coherent capture and emission of carriers by localized impurity orbitals. Since a carrier can be trapped in a localized impurity orbital for a certain time interval , such process has profound influence on the non-equilibrium distribution function. It was proved [75] that such process provides a new mechanism of carrier population inversion, which explains the origin of far-infrared lasing from strained p -Ge [76].

In connection to the possible THz radiation from Si/SiGe quantum wells, such resonant states were studied in [77]. It was found that the width of the resonant level is very sensitive to the position of the impurity when the impurity is moved from the center of the well into the barrier. Therefore, in a δ-doped quantum well sample, the electron transport parallel to the interfaces will depend on the position of the δ-doping. This effect should also depend on the strength of an applied electric field which can inject hot carriers into the resonant states. The study of the hot carrier mobility or drift velocity in a δ-doped quantum well can give us valuable information on the characteristic features of resonant states.

In earlier works on carrier mobilities, one usually took only the conventional Coulomb scattering channel (CCS) channel by impurity ions into account. The presence of resonant states opens another impurity scattering channel which we call resonant state scattering (RSS) channel. How the RSS channel will affect the carrier mobility is still an open question. Experiments on bulk doped semiconductors can hardly provide the answer. Resonant states can also be formed in a doped quantum well in which the impurity levels attached to a higher sub-band

will be degenerate with the 2D continuum of the lower sub-band. A resonant state is then formed through hybridization of these two degenerate states, and the resulting energy level has a certain width. It is important to determine this width in order to consider the effects of the coupled impurity states on the optical and electrical properties of modulation-doped quantum wells.

In this thesis, we have performed Monte Carlo simulations on the hot carrier drift velocity in a δ-doped Si/SiGe quantum well, taking into account all important scattering mechanisms including both the CCS channel and the RSS channel of the impurity scattering. We used a non-variational method outlined in Ref. [77] to obtain energy levels and wave functions of shallow donors. In this approach, the total Hamiltonian is expanded in a complete basis of quantum well eigenstates,

$$H = \left[-\frac{\hbar^2}{2} \frac{\partial}{\partial z} \frac{1}{m_\perp(z)} \frac{\partial}{\partial z} + \frac{1}{m_{||}(z)} \nabla^2_{2D} \right] + V(z) + V_c(\mathbf{r}) \tag{3.1}$$

Here $V(z)$ is the quantum well potential profile and $V_c(\mathbf{r})$ the impurity potential which is taken as the Coulomb potential. This turns the Schrödinger equation into a matrix eigenvalue problem, which is diagonalized to yield all localized, hybridized, and continuum states. The approach has several benefits over the variational method. First of all, no assumptions are made regarding the form of the impurity wave functions, but instead the correct envelope function obtained, which then can be employed for calculating optical matrix elements. In addition, the difference in the effective mass in the well and barriers is easily included, as well as an electric field, and we are able to consider anisotropic materials such as Si and Ge. It is furthermore possible to place the impurities in the barrier instead of in the well, and we thus have a unified approach for treating impurities in modulation-doped hetero-structures. The diagonalization of the matrix problem provides the energies of all eigenstates of the Hamiltonian in Eq. (3.5), and the corresponding eigenvectors allow us to evaluate the wave functions and hence matrix elements such as optical dipole-interaction strengths. In our work, we have particularly focused on the lowest antisymmetric impurity state. This state has been shown to be attached to the second QW sub-band, and for narrow well widths it becomes resonant with the continuum of the first (lowest) sub-band [47, 48]. Any state appearing in the energy region below the lowest QW level must be localized. The lowest one will be the impurity ground state. There are several states attached to the lowest sub-band, and they form what resembles a Rydberg series, with decreasing binding energies converging towards the lowest sub-band edge. Actually, such series of localized states appear below each sub-band, i.e., each QW level has a set of impurity states attached to it . The binding energy of a localized state is therefore to be understood as the smallest energy required to place an initially localized electron into the corresponding QW sub-band.

As long as the impurity is placed in the center of the well, no hybridization or coupling can take place between impurity states that are resonant with sub-bands

of opposite parity. Coupling will however be present as soon as any asymmetry that breaks the parity conservation is introduced such as shifting the impurity position or applying an electric field. The localized state is then 'diluted' throughout a band of actual stationary states, whose profile is represented by a Lorentzian resonance curve [32].

The system for which we will perform the Monte Carlo simulation is a simplified quantum well MODFET structure. The experimentally often-used continuously doped supply region is replaced by a δ-doping layer, separated by an undoped spacer from the active layer, which consists of a Si quantum well (QW), grown between infinitely wide $Si_{1-x}Ge_x$ barriers.

The quantum well is strained due to the lattice mismatch between the Si and the SiGe layers. In result, the degeneracy of the six Δ valleys (the conduction band minima) is lifted. For (001)-grown layers, the two $\Delta_\perp$ valleys, perpendicular to the QW interfaces, will be the lowest conduction-band valleys, strain-split from the four $\Delta_{||}$ valleys by an amount large enough (about 0.7 eV) that the latter valleys can be disregarded altogether [78]. This valley splitting has important consequences for the transport properties of Si/SiGe structures, as will be discussed in Section 3.1. Apart from that, the strain effect is incorporated into the band offset U, which makes up the dominating part of the potential profile $V(z)$ for the conduction band edge.

We will work entirely within the effective-mass approximation. The effective mass $m_{||}$ for the electron motion in the xy-plane is considered to be constant, while the effective mass $m_\perp$ along the growth direction is spatially dependent. Since there is no confining potential in the QW plane, the electrons will propagate as plane waves, accelerated by the applied electric field. The electron states in the conduction band can thus be written as

$$\psi_{\lambda\mathbf{k}}(\mathbf{r}, z) = \frac{1}{L} e^{i\mathbf{k}\cdot\mathbf{r}} \, \varphi_\lambda(z), \tag{3.2}$$

with energies

$$E_{\lambda\mathbf{k}} = E_\lambda + E_\mathbf{k}. \tag{3.3}$$

The index λ enumerates the quantum well levels, $\mathbf{r}$ is the radial vector in the xy-plane, and $\mathbf{k}$ the 2D wave vector for the in-plane motion. We apply periodic boundary conditions in the xy-plane, the area of which is $A = L^2$.

Although the non-parabolicity of the QW sub-bands may be rather strong in Si/SiGe systems, [79] we shall for simplicity assume a parabolic and isotropic conduction-band dispersion relation

$$E_\mathbf{k} = \frac{\hbar^2 k^2}{2m_{||}}. \tag{3.4}$$

The energies E_λ and the wave functions $\varphi_\lambda(z)$ are the solutions of the one-

dimensional QW Schrödinger equation

$$H = \left[-\frac{\hbar^2}{2} \frac{\partial}{\partial z} \frac{1}{m_\perp(z)} \frac{\partial}{\partial z} + V(z) \right] \varphi_\lambda = E_\lambda \varphi_\lambda. \tag{3.5}$$

When the doping concentration is large enough to produce band bending, this effect is incorporated in $V(z)$, and Eq. ((3.5)) is then solved self-consistently together with the Poisson equation, using standard methods.

In the following section we shall use these solutions to calculate all scattering matrix elements. In this way, we can perform a Monte Carlo simulation which takes proper account of the two-dimensional nature of the electronic states in the quantum well.

3.1 Scattering mechanisms

The relevant phonon branches for energy relaxation in the conduction band of Si are inter-valley phonons, since scattering by intra-valley optical phonons is forbidden by symmetry [80, 19].

The inter-valley scattering in Si can be characterized as zero-order optical and first-order acoustic processes, respectively [80, 81]. These labels are derived from the assumed form of the respective interaction Hamiltonians (see below), rather than any physical interpretation of the corresponding vibrational modes. In order to account for the experimentally observed temperature-dependence of the mobility in bulk Si, one generally includes three g (scattering between opposite Δ valleys) and three f (non-opposite valleys) processes [82, 83]. However, as mentioned in the previous section, the electron transport in a strained Si quantum well can be considered to take place only in the two $\Delta_\perp$ valleys, and hence only g processes are possible. The resulting reduction of inter-valley scattering, together with the low in-plane effective mass in the $\Delta_\perp$ valleys, are considered to be the reasons for the very high calculated and observed electron mobility in modulation-doped Si MODFETs [84, 85].

In addition to the inter-valley phonons, we will also include a number of elastic – or approximately elastic – scattering mechanisms, which thus only contribute to the momentum randomization. Besides intra-valley acoustic phonons, we also consider impurity scattering through two separate channels (ionized impurity scattering and resonant scattering), and interface roughness scattering. The results obtained considering all these scattering mechanisms are presented in Papers I and II.

The Monte Carlo approach for solving the Boltzmann transport equation is naturally valid under the same conditions as the Boltzmann equation itself. This means that all scattering events are assumed to occur instantaneously. The internal processes of the collision events themselves are of no importance, and we are therefore able to calculate the transition rate (probability per unit time) $W_{\lambda\lambda'}^{\mathbf{kk}'}$

between well-defined initial $\psi_{\lambda\mathbf{k}}$ and final $\psi_{\lambda'\mathbf{k}'}$ states using the Fermi Golden Rule

$$W_{\lambda\lambda'}^{\mathbf{k}\mathbf{k}'} = \frac{2\pi}{\hbar} \left| M_{\lambda\lambda'}^{\mathbf{k}\mathbf{k}'} \right|^2 \delta(E' - E - \delta E), \tag{3.6}$$

where δE is the amount of energy gained or lost in an inelastic process, and E and E' are simplified notations for the energies of the initial and final (primed) states, respectively. The scattering matrix element $\left| M_{\lambda\lambda'}^{\mathbf{k}\mathbf{k}'} \right|^2$ for each particular scattering mechanism will be derived in the following sections.

The δ-function in Eq. ((3.6)) ensures energy conservation; momentum conservation is however less strict in 2D than in 3D, since the momentum component parallel to the QW growth direction is not conserved. In result, phonons (both for elastic and inelastic mechanisms) may be emitted and absorbed with any momentum, as long as the in-plane component is conserved. The various phonon modes are however independent of each other, and it therefore suffices to sum the final transition probabilities corresponding to each particular value of the momentum of the emitted/absorbed phonon.

The total scattering rate $W_\lambda^{\mathbf{k}}$, i.e. the probability per unit time to be scattered out of a state $\psi_{\lambda\mathbf{k}}$ by a particular mechanism, is obtained by summing over all possible final states:

$$W_\lambda^{\mathbf{k}} = \sum_{\lambda'\mathbf{k}'} W_{\lambda\lambda'}^{\mathbf{k}\mathbf{k}'} \tag{3.7}$$

Using the periodic boundary conditions, the summation over $\mathbf{k}' = (k', \theta_{\mathbf{k}'})$ can be converted into a double integral. The parabolic dispersion relation (3.4) gives the familiar constant density of states in a 2DEG

$$\rho_\lambda(E) = \frac{m_{||}}{2\pi\hbar^2} \Theta(E - E_\lambda), \tag{3.8}$$

where the step-function $\Theta(x)$ indicates the absence of states below the sub-band edge E_λ. Eq. ((3.8)) gives the density of states per spin (and valley); none of the scattering processes we will consider have the ability to flip the spin polarization.

We can now use Eq. ((3.8)) to turn the integration over k' into integration over E', and thereby obtain

$$W_\lambda^{\mathbf{k}} = \frac{2\pi}{\hbar} \frac{m_{||}}{\hbar^2} \frac{L^2}{(2\pi)^2} \sum_{\lambda'} \int_{E_{\lambda'}}^{\infty} dE' \int_0^{2\pi} d\theta_{\mathbf{k}'} \left| M_{\lambda\lambda'}^{\mathbf{k}\mathbf{k}'} \right|^2 \delta(E' - E - \delta E). \tag{3.9}$$

The integration over energy is more or less trivial, due to the δ-function, and the angular integral can, depending on the particular scattering mechanism, often be evaluated analytically. Note how the lower limit of integration over the energy E' takes into account the vanishing density of states below the corresponding sub-band bottom $E_{\lambda'}$.

3.2 Monte Carlo model details

The two commonly used approaches for Monte Carlo simulations in semiconductors are single-particle and ensemble simulations. If the system to be investigated exhibits strong carrier-carrier correlation, or involves a time dependent response to an external stimulation, it is necessary to use the ensemble Monte Carlo approach. However, we will study the transport properties of independent carriers in semiconductors under an applied homogeneous electric field. Although several different scattering mechanisms are taken into account, we do not include carrier-carrier correlation nor impact ionization. Hence, it is proper to use the standard single-particle Monte Carlo technique which was developed for carrier transport in semiconductors [7]. There are two methods to calculate the drift velocity of the carriers. One can first simulate the carrier distribution function in momentum space, and then average the momentum with this distribution to obtain the velocity. One can also simulate the drift velocity directly without using the distribution function; that is the approach we have adopted, and thus we simulate the distribution function and the drift velocity simultaneously. In this way it is possible to use the distribution function to check the convergence of the simulation. Furthermore, without any applied electric field the distribution function is spherically symmetric due to thermalization, but will become asymmetric when the field is turned on. Such information of the distribution function stretching along the field direction will be very useful for the understanding of the calculated drift velocity. Because our Monte Carlo simulation includes inter-valley scattering, it is necessary to specify the electron eigenstate $\psi_{\lambda \mathbf{k} j}$ in a Si/SiGe quantum well by the sub-band index λ , the 2D wave vector $\mathbf{k}$, and the valley index j. Because the bulk symmetry is broken in layer structures, in a Si/SiGe quantum well there are only two low-lying valleys to take into account [78]. Under an applied dc electric field $\mathbf{F}$ parallel to interfaces, an electron will perform free-flight motion between two collisions. During the free flight motion only the wave vector $\mathbf{k}$ changes with time; specifically, it evolves linearly as the carrier is accelerated by the field. Conversely, when an electron is scattered by one of the various scattering mechanisms, its state changes instantaneously from $\psi_{\lambda \mathbf{k} j}$ to $\psi_{\lambda' \mathbf{k}' j'}$. We will label the free-flight time intervals by l, and specify the lth time interval as from $t_{l,i}$ to $t_{l,f}$. Let $\mathbf{v}_l(\mathbf{k}(t))$ be the velocity during the free flight in the time interval l. Then the drift velocity $\mathbf{v}_{dr}(\varepsilon)$ is calculated as [7]

$$\mathbf{v}_{dr}(\varepsilon) = \frac{1}{T} \sum_l \mathbf{v}_l[\mathbf{k}(t)]dt \tag{3.10}$$

where $T = \sum_l (t_{l,f} - t_{l.i})$ is the total duration of the Monte Carlo simulation.

To perform the Monte Carlo simulation, we keep track of the momentum changes during each free flight, and then take a proper average. In practice it is more convenient to average over the energy. We will simplify the notation by

defining $k_{l,i} = k(t_{l,i})$ and $k_{l,i} = k(t_{l,i})$ as the initial and final wave vectors of the free-flight interval l, and we also introduce $K = e\varepsilon T/\hbar$. Using the relation

$$V_{\lambda j}(\mathbf{k}) = \frac{1}{\hbar}\nabla_k E_{\lambda,j(\mathbf{k})} \tag{3.11}$$

where $E_{\lambda,j}(\mathbf{k})$ is the 2D sub-band energy with explicit reference to the jth valley, we can rewrite Eq. (3.10) as

$$\begin{aligned} \mathbf{v}_{dr}(\varepsilon) &= \frac{1}{K}\sum_l \int k_{l,i}k_{l,f}\frac{1}{\hbar}\nabla_k E_{\lambda(l),j(l)}(\mathbf{k})d\mathbf{k} \\ &= \frac{1}{\hbar K}\sum_l [E_{\lambda(l),j(l)}(\mathbf{k}_{l,f}) - E_{\lambda(l),j(l)}(\mathbf{k}_{l,i}), \end{aligned} \tag{3.12}$$

where we have explicitly indicated that both the sub-band and valley index are functions of the interval label l. When using this equation to simulate the drift velocity for different temperatures under various applied electric fields, the convergence of the Monte Carlo results presented below has been checked carefully. To produce the Monte Carlo numerical results, we first derive the eigensolutions from the Schrödinger equation (3.5) in a Si/Si_xGe_{1-x} quantum well using well-known values of the electron effective mass, band offsets, and deformation potentials [78]. The details of the calculation can be found in Ref [77]. With these eigensolutions one can calculate all the relevant scattering rates given in the preceding section, and the Monte Carlo calculation can then be performed.

Chapter 4

Electronic transport in SSL in the Wannier-Stark regime

Let us consider a semiconductor superlattice subject to an electric field **F** along the growth direction z. We will assume that a semiclassical description is sufficient. If an electron does not suffer any scattering it will execute a periodic motion in real space, and if **k** is restricted to the first Brillouin zone the motion will be periodic in **k** space as well, and the period is $\omega_B = edF/\hbar$. If now scattering events are taken into account, the behavior will be altered, and evidently the cross-over is expected to take place when the scattering relaxation time τ is of the same order as the reciprocal BO frequency $1/\omega_B$. It is thus convenient to introduce a threshold field F_0 such that $F_0 = \hbar/ed\tau$.

For a weak field $F \ll F_0$ the electron cannot complete even one cycle of BO before being scattered, and hence its transport properties can be described in terms of a drift velocity. This drift velocity increases with the electric field strength. In the high-field limit $\omega_B\tau \gg 1$, an electron can perform many cycles of BO without suffering a scattering. In this case the Bloch electrons can hardly contribute to the net charge transport, and consequently the drift velocity of electrons in a SSL approaches zero. As a result, the negative differential drift velocity appears in the high-field regime $F \gg F_0$. In a bulk crystal the lattice constant is so small that the corresponding threshold field F_0 is too high to be achieved in reality. The large value of the periodicity d in SSL samples provides the possibility to observe the BO and related physical properties. Many experiments [58, 61, 62, 71, 86] have indeed confirmed the existence of BO in SSL at low temperatures as well as at room temperatures. Shortly after the proposal of Esaki and Tsu [12], there appeared a theoretical study [66] on the interaction between a weak field of terahertz frequency and the electrons in a SSL miniband performing BO with allowed energy relaxation. It was suggested that such an interaction can

lead to an amplification of the THz field in the region of frequency less than the BO frequency ω_B, and the amplification curve exhibits a resonance like structure around $\omega \simeq \omega_B$. An extension of the weak-field theory [66] of amplification to the case of a strong THz field [87, 88, 68] indicated the possible resonant amplification of THz fields at $\omega = n\omega_B$ with integer n.

With increasing strength of **F**, the quasi-classical method becomes less reliable and one needs a full quantum mechanical approach. The analytical solution of Wannier [16] proves that the energy spectrum of a Bloch electron under an external dc field **F** consists of an infinite series of eigenvalues which are equally separated by an energy difference $eFd = \hbar\omega_B$. This series of eigenenergies is called the Wannier-Stark ladder (WSL). The corresponding eigenfunctions are also equally displaced by a distance d in real space along the field direction. In a realistic SSL sample, the levels in a WSL are broadened by scatterings. Under a weak field **F**, the small energy separation eEd is smeared out by scatterings, and so the quasi-classical energy band description is a good approximation.

In this chapter, the electron transport in SSL under an applied dc electric field, driven by the scattering-assisted electron transitions between neighboring WSL levels, is studied with a Monte Carlo approach. To provide a complete picture of the physical phenomenon, we investigate the combined effect of optical phonon scattering, acoustic phonon scattering, and elastic alloy disorder scattering. We analyze the contribution of each scattering mechanism to the total current, as well as effect of each scattering mechanism on the carrier distribution function. Our calculated field dependence of the drift velocity will be compared with the data obtained recently from the experiments on time-domain THz spectroscopy of an AlGaAs/GaAs SL [17]. These experiments provide a method to determine the electric field dependence of the drift velocity of carriers in undoped SSL.

We will investigate the carrier transport along the SSL growth direction for the electric field strength F where system exhibit negative deferential conductivity. In this case the semiclassical theory is no longer valid and carrier transport occurs via scattering assisted hops between the WSL states $\psi_i(z)$ localized in different SSL unit cells. In a GaAs/AlGaAs SSL the essential scattering mechanisms are the alloy disorder scattering, the polar optical phonon scattering, and the acoustic scattering due to both the deformation potential and the piezoelectric interaction. To study the scattering-assisted electron transport between WSL levels in a semiconductor superlattices under an external dc field, in order to reach high quantitative accuracy, we must use the electron eigensolutions to calculate the matrix elements of all scattering processes. If the electric field F is not extremely strong so as to cause Zener tunneling, the eigensolutions of the WSL levels can be derive with a well-established computation scheme [15].

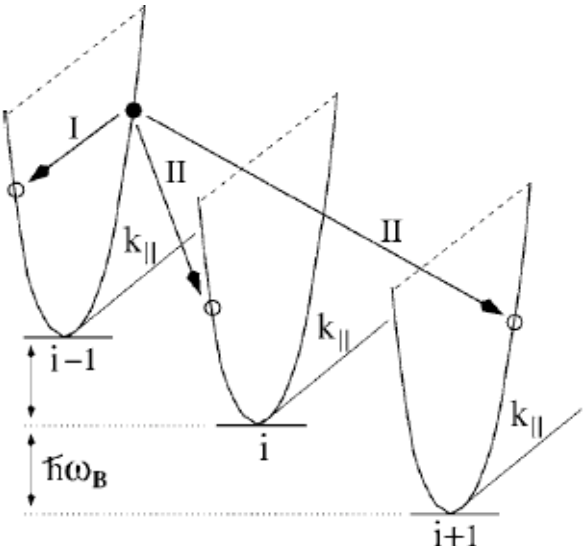

Figure 4.1: A schematic illustration of the scattering-induced hopping transport in a biased SSL in the WSL regime (Paper III)

4.1 Transport in SSL as scattering-assisted carrier hopping

The scattering-assisted carrier hopping is illustrated schematically in Fig. 4.1, where the positions of the unit cells in the SSL are marked as $i-1, i, i+1, i+2, \cdots$ The WSL levels E_z^i are attached to these unit cells as indicated by horizontal lines, together with a series of two-dimensional energy dispersions $\epsilon_{k_{||}}$. We notice that the WSL levels E_z^i are equally separated by the BO energy $\hbar\omega_B$. A carrier that occupies its initial state $\Psi_{ik_{||}}(r)$ marked by the solid dot in Fig. 4.1 can either be scattered into the states at the same WSL energy level E_z^i this intra-level scattering is indicated in Fig. 4.1 as process I , or it can hop to the state $\Psi_{jk_{||}}(r)$ associated with another WSL energy level E_z^j with $i \neq j$ (this inter-level scattering is indicated in Fig. 4.1 as process I). The intra-level scattering cannot produce a finite current, but can significantly affect the distribution function over the two-dimensional momentum $k_{||}$. In the presence of a strong electric field, the electron system in a SSL can be viewed as a number of quasi-two-dimensional electron ensembles, each of which is localized in one SSL unit cell. These ensembles are coupled by the inter-level scattering mechanisms to be introduced below. The hopping of electrons can occur via the emission or absorption of phonons as well as by elastic alloy disorder scattering. The rates of various scattering processes

between $\Psi_{ik_{||}}(r)$ and $\Psi_{ik'_{||}}(r)$ depend on the applied field strength and the temperature. As an example to clarify this point, let us assume a small momentum component $k_{||}$ of the electron in its initial state $\Psi_{ik_{||}}(r)$ such that the associated kinetic energy $\varepsilon_{k_{||}}$ is less than the BO energy $\hbar\omega_B$. This is usually the situation if the applied electric field is strong and the temperature is not too high. Via the emission of phonons or by elastic scattering the electron can hop to the state $\Psi_{ik_{||}}(r)$ only if $j > i$. Such inter-level scattering processes are marked in Fig. 4.1 as process I. Inter-level scattering via the absorption of phonons can be significant only at high temperatures. Inter-level scattering will produce a drift electric current flowing through the SSL. In our numerical calculations of this current, all inter-level scattering-assisted transport processes are included.

We would like to point out that a similar mechanism of scattering-assisted hops between unit cells in a disordered SSL in the absence of an external electric field has been studied [89]. However, since there is no electric driving force, the electron transport has the character of diffusion rather than drift, and there is no net current flow. It is important to emphasize here that in our study the electric field strength is not extremely high so as to cause Zener tunneling. Hence, the scattering-assisted hops are restricted within the WSL associated with one miniband.

Chapter 5

Lattice (TD)DFT applied to disordered and correlated systems and quantum transport

5.1 Introduction

5.1.1 Time Dependent Quantum Transport (TDQT)

Recently emerged molecular electronics [90] requires thorough research on transport phenomena of the systems containing molecular device attached to two metallic leads. Quantum transport theory should be able to take into account all the details of the molecular subsystem (which contains either single or very few molecules) and of the junction between molecular device and bulk leads. The reasonable choice will be to start with DFT which provides the knowledge of atomistic details with very good accuracy.

Since the pioneering work by Lang and collaborators [91, 92], density-functional theory in the adiabatic local density approximation (ALDA) has become a standard method for describing steady transport of nanoscopic devices or molecules attached to macroscopic leads [93, 94, 95, 96]. The ALDA is strictly an effective one-body scheme and does not *per se* require any many-body techniques, but it has proved convenient to use the machinery of non-equilibrium Green function theory (NEGF) [97, 98] to treat the effects of the leads on the central device.

A problem of great interest is also how a steady state is established after an external bias has been applied. It is then necessary to follow the temporal evolution

when a system initially in equilibrium is exposed to external fields.

The conceptually simplest method is to consider large but finite external electrodes with an initial charge unbalance [99, 100, 101, 102, 103, 104]. With finite but large leads, a true steady state will not exists but rather a long-lived plateau when initial transients has decayed but when the electrodes are not yet discharged. The method with finite but large electrodes has also been applied to ultra-cold atoms in 1D optical lattices [105].

Alternatively, one may consider a finite central region connected to semi-infinite macroscopic leads [106, 107, 108, 109, 110]. The entire system is initially in equilibrium, and at a certain time a possibly time-dependent bias is applied. The time evolution is usually obtained via NEGF via the Kadanoff-Baym (KBE) equations [97], also in one-particle schemes like ALDA where it is strictly speaking not necessary. Within NEGF one can also go beyond effective one-particle schemes and consider a variety of many-body approximations [110, 111, 112]. This method has also been used to describe the nuclear motion in nanodevices [113].

In the works on transport in this thesis, density-functional theory in its static and dynamic form has been the key method. In the following pages I present brief summaries of the key ideas in density-functional theory and in the model Hamiltonians used.

5.1.2 General aspects of Density Functional theory (DFT)

Density functional theory (DFT) is one of the most widely used and successful quantum mechanical tool for determining the electronic structure of solids. The most important properties (e.g., binding energy in molecules, band structures of solids, etc.) can be obtained with very good agreement with experiments.

Historically, the first theory replacing the wave function by the electronic density was developed in the 1920's by Thomas and Fermi (TF). The TF theory has not become popular since it was shown, short after its formulation and application to atoms, that it could not describe molecular bonding. For a long time, density-functional theory was not used much and was more considered as a model or crude approximation. Density-functional theory became really important when it was put on a firm basis by Hohenberg and Kohn [114], and when the equivalent one-particle scheme which handles the kinetic energy functional exactly was invented by Kohn and Sham (KS) [115]. In the KS scheme, the large terms representing the kinetic energy, interaction with the lattice potential, and the classical Coulomb energy are all treated exactly, and one has to introduce approximations only for the much smaller contributions from exchange and correlation. Already the simplest local-density approximation (LDA) is quite successful for obtaining, say, cohesive energies, lattice constants and vibronic frequencies from first principles with e^2 and $\hbar$ as the only input parameters.

The aim of DFT is to reformulate quantum mechanics so that the quantity of interest is not the many-body wave function $\Psi(\mathbf{r}_1, \mathbf{r}_2, ..., \mathbf{r}_N)$ depending on $3N$ co-

ordinates but the single particle density $n(\mathbf{r})$ depending on only three coordinates. This is of course an enormous simplification.

Hohenberg and Kohn considered systems with N particles interacting via a given fixed interaction $v_c(\mathbf{r})$ but subject to different external one-body potentials $v(\mathbf{r})$,

$$H = \sum_i^N -\frac{1}{2}\nabla_i^2 + \frac{1}{2}\sum_{i\neq j}^N v_c(\mathbf{r}_i - \mathbf{r}_j) + \sum_i^N v(\mathbf{r}_i) = \hat{T} + \hat{U} + \hat{V}_{ext} \tag{5.1}$$

The second line of the equation above defines three energy operators, which in turn define three contributions to the total energy,

$$E = T + U + V_{ext} \tag{5.2}$$

Keeping the interaction fixed, the ground-state energy can be considered a functional of the external potential,

$$E = E[v] \tag{5.3}$$

In the same way, the ground-state density depends functionally on v, $n(\mathbf{r}) \equiv n[v;\mathbf{r}]$. Hohenberg and Kohn were then able to show that the mapping from v to n is invertible, or more precisely, that if two ground-state densities $n(\mathbf{r})$ and $n'(\mathbf{r})$ are equal, then the corresponding potentials $v(\mathbf{r})$ and $v'(\mathbf{r})$ agree up to a constant, $v'(\mathbf{r}) = v(\mathbf{r}) + C$. (The constant C may be fixed by e.g. requiring that the potential tend to zero at far distances.) This means that we may use n in place of v as the fundamental variable. From first-order perturbation theory follows that

$$\frac{\delta E[v]}{\delta v(\mathbf{r})} = n(\mathbf{r}), \tag{5.4}$$

and if we just solve for v and insert $v[n;\mathbf{r}]$ in Eq. (5.3) we would loose information since n is the functional derivative with respect to v. Instead, HK defined the basic density-functional $F[n]$ as a Legendre transform,

$$F[n] = E[v] - \int d^3r \frac{\delta E[v]}{\delta v(\mathbf{r})} v(\mathbf{r}) = E[v] - \int d^3r\; v(\mathbf{r}) n(\mathbf{r}). \tag{5.5}$$

In 1979, Levy [116] gave a very nice alternative definition of the density functional $F[n]$ based on restricted search. He considered the expectation values $E[\Psi] = \langle\Psi|\hat{T} + \hat{U}|\Psi\rangle$ for a subclass of wave functions which correspond to a given density profile $n(\mathbf{r})$. Such expectation values can clearly be considered as a functional of Ψ, and it is certainly bounded from below. Such functionals may not always have a minimum, but the infimum always exists. Levy defined the density functional as

$$F[n] = \inf\langle\Psi|\hat{T} + \hat{U}|\Psi\rangle, \tag{5.6}$$

and showed that it is equivalent with the original HK definition whenever the latter exists.

To be useful, density-functional theory should provide means for obtaining all ground-state properties without referring the underlying many-body wave function. To this end, HK introduced a functional $E_v[n]$ depending on *two* variables, n and v,

$$E_v[n] = F[n] + \int d^3r\; n(\mathbf{r})v(\mathbf{r}). \tag{5.7}$$

They showed that the ground-state density corresponding to a given external potential v can be obtained by minimizing $E_v[n]$ with respect to n while keeping v fixed, and that the corresponding ground-state energy is

$$E[v] = \min_n E_v[n] \tag{5.8}$$

at constant particle number N.

If we go back to the total ground-state energy in Eq. (5.2), the terms T, U, and V_{ext} are all quite large. The interaction energy with the external potential is trivial, $V_{ext} = \int nv$. In the interaction energy we may split of the large classical Coulomb energy

$$E_H[n] = \frac{1}{2}\int d^3r\; d^3r'\; v_c(\mathbf{r}-\mathbf{r}')n(\mathbf{r})n(\mathbf{r}'), \tag{5.9}$$

which leaves the much smaller exchange-correlation part $U_{xc} = U - E_H$ to be approximated. However, the kinetic energy is not known as an explicit density functional even for non-interacting fermion. The difficulty to treat the kinetic energy accurately was a major limitation of the early Thomas-Fermi theories. Kohn and Sham invented an algorithm whereby the largest contribution to T, namely the corresponding kinetic energy for *non-interacting* particles, $T_0[n]$, may be constructed in a numerically exact way. In this way, only $E_{xc} = U_{xc} + T_{xc}$ needs to be approximated (T_{xc} is the exchange-correlation contribution to the kinetic energy).

Kohn and Sham decompose the density-functional in three terms,

$$F[n] = T_0[n] + E_H[n] + E_{xc}[n] \tag{5.10}$$

The minimization in Eq. (5.8) leads to

$$\frac{\delta T_0[n]}{\delta n(\mathbf{r})} + v_H(\mathbf{r}) + v(\mathbf{r}) + v_{xc}(\mathbf{r}) = \mu, \tag{5.11}$$

where $v_H(\mathbf{r}) = \delta E_H/\delta n(\mathbf{r})$ is the electrostatic potential from the ground-state electron distribution $n(\mathbf{r})$, and where

$$v_{xc}(\mathbf{r}) = \frac{\delta E_{xc}[n]}{\delta n(\mathbf{r})} \tag{5.12}$$

describes the corrections from exchange and correlation. The parameter μ is a Lagrange parameter corresponding to the constraint $N = \int n = const.$ Now, independent-particle theory can also be density-functionalized, which leads to the minimization of

$$E_v^{(0)}[n] = T_0[n] + \int d^3r\; n(\mathbf{r}) v_{eff}(\mathbf{r}) \tag{5.13}$$

when the independent-electron system is put in an external potential v_{eff}. The corresponding Euler equation reads

$$\frac{\delta T_0[n]}{\delta n(\mathbf{r})} + v_{eff}(\mathbf{r}) = \mu_0, \tag{5.14}$$

The unknown $T_0[n]$ enters in both Euler equations, Eqs. (5.14, 5.14). However, for independent particles we may evaluate the kinetic energy via the corresponding one-electron orbitals, *i.e.*,

$$T_0[n] = \sum_0^{occ} \langle \phi_\nu | -\frac{\nabla^2}{2} | \phi_\nu \rangle \tag{5.15}$$

Comparing Eqs.(5.11) and (5.14) we see that we may solve the original problem of interacting electrons in Eq. (5.8) by solving orbital equations

$$\left[-\frac{1}{2}\nabla^2 + v_{eff}(\mathbf{r}) \right] \phi_\nu = e_\nu \phi_\nu \tag{5.16}$$

$$n(\mathbf{r}) = \sum_1^{occ} |\phi_\nu(\mathbf{r})|^2 \tag{5.17}$$

self-consistently ($v_{eff} = v_H + v + v_{xc}$). When self-consistency has been achieved, $T_0[n]$ has been obtained exactly for the density profile n.

The orbital eigenvalues e_ν have no simple physical meaning except the uppermost occupied one which equals the ionization energy or chemical potential [117]. However, they are useful auxiliary quantities for constructing T_0 and thereby the total energy. For independent particles, we have

$$E_v^{(0)}[n] = T_0[n] + \int d^3r\; n(\mathbf{r}) v_{eff}(\mathbf{r}) = \sum_1^{occ} e_\nu \tag{5.18}$$

which gives

$$T_0[n] = \sum_1^{occ} e_\nu - \int d^3r\; n(\mathbf{r}) v_{eff}(\mathbf{r}). \tag{5.19}$$

Thus, the ground-state energy of the interacting system may be written

$$E[n] = \sum_1^{occ} e_\nu + E_H[n] + E_{xc}[n] + V_{ext} - \int d^3r\; n(\mathbf{r}) v_{eff}(\mathbf{r}) \tag{5.20}$$

at self-consistency. Here $v_{eff} = v_H + v + v_{xc}$ as before.

The exact functional E_{xc} is in general highly unknown and approximations must be introduced. The simplest and most popular of these approximations is the so-called local density approximation (LDA). It consists in approximating the functional by basing it on a simpler reference system where it is a known quantity. The reference model to be considered can be different depending on the actual system under consideration. In *ab initio* DFT, the interacting homogenous electron gas is used as such a model system. In this case, to proceed in the LDA, one calculates the total energy E, the single-particle kinetic energy T_0, and then finds E_{xc} by

$$E_{xc} = E - T_0 - E_H. \tag{5.21}$$

In this way, one can formulate the exchange-correlation energy as functional of the electron density, and this can be used to calculate the $v_{xc}[n](r)$ assuming that it is a local functional of the density:

$$v_{xc}[n](r) \approx v_{xc}^{LDA}(n(r)), \tag{5.22}$$

where, as said above, the function $v_{xc}^{LDA}(n)$ is found from the reference system (the homogenous electron gas). With this v_{xc}, on can then solve the Kohn-Sham equations, and calculate the total energy and other observables of interest. Although the LDA is a first hand approximation for inhomogeneous system (for example, molecules, crystalline solid alloys, etc.) it has been incredibly successful for predicting the ground-state properties of these systems [118].

5.1.3 General aspects of Time Dependent DFT

The knowledge of the ground state density provides a lot of information about the system under investigation, but is not sufficient if one wants to obtain quantities like electron addition or electron removal energies, excitation energies in general, etc. Dynamical effects, e.g. the transport properties of a given system, are out of the scope of such ground state approaches.

The dynamical effects can be studied by exposing the system to a time dependent external potential and calculating the evolution of the density in time, the method we use in Paper IV.

Obtaining such time-dependent quantities has become possible thanks to the time-dependent formulation of DFT, Time-Dependent Density-Functional Theory (TDDFT), which was put on rigorous grounds with a theorem by Runge and Gross (RG) [119]. In essence, the RG theorem deals with the time-evolution of a system as induced by a time-dependent scalar potential. The initial state of the system has not necessarily to be the ground state. In the original formulation, the external potential $v(\mathbf{r}, t)$ was assumed to be expandable into a Taylor series with respect to the time coordinate around the time origin t_0. In principle, the assumption

of an analytic v is rather restrictive, and more recent formulations release such a hypothesis.

The RG theorem states that if two systems start to evolve in time from the same initial state, and at all later times have the same time-dependent density $n(\mathbf{r},t)$, then the corresponding external potentials are equal up to a time-dependent constant $C(t)$. That is,

$$n_1(\mathbf{r},t) = n_2(\mathbf{r},t) \Leftrightarrow v_1(\mathbf{r},t) = v_2(\mathbf{r},t) + C(t) \tag{5.23}$$

The original RG proof was based on performing time derivatives of progressively increasing order, and showing that the power series expansion of $n_1(\mathbf{r},t)$ and $n_2(\mathbf{r},t)$ differ when $v_1(\mathbf{r},t) \neq v_2(\mathbf{r},t) + C(t)$.

In the treatment by Runge and Gross, a stationary action principle is considered for TDDFT, based on the quantum mechanical action

$$A[n] = \int_{t_0}^{t_f} dt \left\langle \Psi(t) \middle| i\frac{\partial}{\partial t} - \hat{H} \middle| \Psi(t) \right\rangle . \tag{5.24}$$

$A[n]$ plays a role similar to the energy functional of ground state DFT (A is a functional of the density n by virtue of the RG theorem). However, the RG variational formulation was later shown to be inconsistent with causality requirements. The issue was then solved moving the formulation to time-domains defined on the Keldysh contour (a more straightforward treatment, which avoids the Keldysh contour, has been provided quite recently).

Finally, in their work, Runge and Gross presented an extension of the Kohn-Sham formalism to time-dependent situations. Similarly to the ground state case, the TDKS equations are single-particle Schrödinger equations with an effective potential which accounts for the effect of the electron-electron interaction. Thus,

$$[-\frac{1}{2}\nabla^2 + v(\mathbf{r},t) + \int d\mathbf{r}' \frac{n(\mathbf{r}',t)}{|\mathbf{r}-\mathbf{r}'|} + v_{xc}(\mathbf{r},t)]\phi_\nu(\mathbf{r},t) = i\frac{\partial}{\partial t}\phi_\nu(\mathbf{r},t), \tag{5.25}$$

and $v_{xc}(\mathbf{r},t)$ is obtained as the functional derivative of the exchange-correlation part of A with respect to the density. To emphasize the similarity with the previous section, we rewrite Equation (5.25) as a time-dependent Kohn-Sham problem

$$\left(\hat{t} + \hat{v}_{KS}(t)\right)\phi_\nu(t) = i\frac{\partial \phi_\nu(t)}{\partial t} \tag{5.26}$$

where $\hat{t} = -\nabla^2/2$. Similarly to the previous section, one defines

$$n(\mathbf{r},t) = \sum_{\nu}^{occ} |\phi_\nu(\mathbf{r},t)|^2 \tag{5.27}$$

where the now time-dependent density is equal to the original density from the fully interacting system.

Thus, in order to obtain the time dependent density $n(\mathbf{r}, t)$ one evolves the Kohn-Sham orbitals. Since the exchange-correlation potential $v_{xc}[n](\mathbf{r}, t)$ depends on both time and space coordinates, it is now a considerably more complicated object than in the ground state case. The extra complication is because the exact potential is not just non-local in space, it is also non-local in time. This non-locality in time is at origin of what is usually referred to as memory-effects. Just like the LDA simplifies the ground-state v_{xc} by assuming that it is a local function of the density, the simplest approximation in TDDFT is the Adiabatic Local Density Approximation (ALDA), which also neglects the memory effects. The ALDA can then be expressed as

$$v_{xc}[n](\mathbf{r}, t) \approx v_{xc}(n(\mathbf{r}, t)). \tag{5.28}$$

Clearly, in this approximation the v_{xc} at a time t and position $\mathbf{r}$ is expressed as a function of the density at the very same point in space and time. The specific form of this function will be the same as the one used for ground state calculations.

We use TDDFT to perform real-time propagation of the KS orbitals. In this way, we are able to address and investigate phenomena such as transient effects in quantum transport, and beyond the linear regime.

Because of the versatility of the (static or time-dependent) density-functional approach, many different kind of systems can be treated. This even permits to explore the properties of lattice models with strong correlation and/or disorder effects. This is done in this thesis, for the specific case of the so-called Hubbard-Anderson model.

5.2 Correlations and disorder effects in condensed matter systems

5.2.1 Anderson localization

Disorder is ubiquitous in nature and often, even if it is only a weak perturbation, it tends to strongly affect the properties of many physical systems. The most celebrated effect of disorder is probably the Anderson localization, i.e. the localization of individual particles or waves in a disordered energetic landscape. This fundamental effect of disorder was already been explored in depth more than 50 years ago, because of the wide interest at that time in the transport of electrons in crystals. These imperfections lead to a dramatic change in the conduction properties of real materials.

It is well known that for crystals, reflections at the potential barriers are very strong even in the absence of disorder. However, extended Bloch states can still

exist, provided that the energies of the individual lattice sites are equal or arranged in a periodic way.

In 1958, Anderson [120] showed that if the on-site energies are instead shuffled in a random way, the reflections interfere destructively and the eigenfunctions of the system become exponentially localized. When the energy or the disorder strength is varied, the system can thus undergo a transition from the metallic phase with delocalized eigenstates to the insulating phase, where the eigenfunctions are exponentially localized:

$$|\psi^2(\mathbf{r})|exp(-|\mathbf{r}-\mathbf{r}_0|/\xi), \tag{5.29}$$

and with ξ is the localization length. The character of this transition remained, however, unclear for about 20 years, until Wegner conjectured, developing earlier ideas of Thouless (1974), a close connection between the Anderson transition and the scaling theory of critical phenomena ([121]). Three years later, Abrahams, Anderson, Licciardello, and Ramakrishnan formulated a scaling theory of localization [122], which describes how the dimensionless conductance g changes with the system size L,

$$d\ln g/d\ln L = \beta(g). \tag{5.30}$$

In lattice systems, the Anderson localization can be investigated in terms of a tight-binding model of disorder originally proposed by Anderson,

$$\hat{H} = -t\sum_{\langle ij\rangle} c_i^\dagger c_j + \sum_i \epsilon_i c_i^\dagger c_j, \tag{5.31}$$

where $\langle ij\rangle$ denotes that the sum is restricted to nearest neighbor sites and the random site energies ϵ_i are chosen from some distribution $P(u)$; the standard choice is the uniform distribution over an interval $[-W/2; W/2]$ (box distribution).

To quantify the degree of localization due to disorder and interactions, we use the inverse participation ratio (IPR) ζ_0. For single-particle states the IPR associated with a given orbital is defined as:

$$\zeta_0 = \sum_i^M n_i^2/(\sum_i^M n_i)^2, \tag{5.32}$$

where $n_i = |\psi_i|^2$ is the density at site i and the sums extend to all the sites M in the system. For completely localized states (when $\psi \neq 0$ at only one site) we get $\zeta_0 = 1$, while ζ_0 is smallest for localized states.

The consequences of electron localization are most pronounced in the transport properties of a disordered system. Localized electrons cannot contribute to transport if the sample is larger than the localization length of the electronic states.

Anderson had predicted that disorder is most effective in systems with a small number of nearest neighbors leading to a small connectivity. Thus it was obvious that localization effects would be most pronounced in low dimensions where the number of nearest neighbors is reduced. It was first argued by Mott and Twose in 1961 [123] that in a one-dimensional system all electron states are localized. To summarize, the first stone was laid down in 1958, and in the following two decades the theory was completed without including interaction effects, culminating in the success of the scaling theory.

In the late eighties and early nineties, the tenets of the scaling theory of disordered systems were challenged by experimental studies [124, 125, 126, 127, 128] of 2D Si MOSFET-samples with low-disorder and in the strongly interacting regime. These experiments showed quite clearly that, in many instances, to describe disordered condensed-matter systems, one needs to fully understand the interplay of disorder and interactions, something which is lacking in the standard scaling theory of Anderson localization. Afterwards, several experiments also made evident that often, when present together, neither disorder or interactions can be considered as a weak perturbation. Instead, they have to be described on equal footing. An important theoretical model providing such a description is the so-called Anderson-Hubbard model, which is investigated in Paper IV and is the subject of the next three sections.

5.2.2 A popular approach to interacting systems: the Hubbard model

The Hubbard model [129] is one of the most studied models in condensed matter theory. Since its inception, it has constantly gained popularity and has been applied in several contexts, thus becoming a truly paradigmatic model to study the effect of strong correlations among the electrons. The Hubbard model was introduced to capture the physics of the competition between delocalization, driven by hybridization, and localization of electrons induced by the electronic interaction. Generally speaking, it is too a simple model to describe accurately any real material. However, it is believed to retain at least the important features of strongly correlated systems and their complex physical properties. Not surprisingly, a vast literature about its physics exists. In the following, we will only briefly summarise the most important aspects of the Hubbard model. Since this thesis focuses on the non-equilibrium behavior of strongly correlated systems, we consider a time dependent-version of the Hubbard Hamiltonian. The latter, in standard notation, reads:

$$\hat{H}(\tau) = -t \sum_{\langle ij\rangle,\sigma} c^{\dagger}_{i\sigma} c_{j\sigma} + \sum_i U_i \hat{n}_{i\uparrow}\hat{n}_{i\downarrow} + \sum_i v_i \hat{n}_i + V_{ext}(\tau), \tag{5.33}$$

where t is the hopping parameter, which is the tunneling amplitude between nearest neighbors sites in the system (these are denoted by $\langle ij\rangle$). The hopping param-

eter is taken to be the same for all the sites in the system, and its value is set to be $t = 1$. Moreover, $\hat{n}_{i\sigma} = c^{\dagger}_{i\sigma} c_{i\sigma}$, with $\sigma = \uparrow, \downarrow$, is the local density operator expressed in terms of electron creation and destruction operators, whilst $\hat{n}_i = \hat{n}_\uparrow + \hat{n}_\downarrow$ is the total density operator. The electron-electron (repulsive) interaction is taken to be local (on-site) and is denoted by U_i. The term $\sum_i v_i \hat{n}_i$ is the on-site energy. Finally, $V_{ext}(\tau)$ is the external potential applied to the system in time dependent calculations (τ is the time-label).

The Hubbard model is the minimal lattice model containing the physics of electron- electron correlations. Nevertheless, its theoretical understanding is still far from being complete. The exact solution has been found for the ground state of the one-dimensional homogeneous system. Here, the model is integrable [130] and the exact ground state could be constructed by using the Bethe Ansatz [131]. The ground state solution for the 1D homogeneous system will be our reference system in the same way as the ground state solution for homogeneous electron gas is used as a reference to build LDA exchange-correlation potentials for 3D continuous systems.

From the exact Bethe-Ansatz solution, it could be proven that in 1D, for any $U > 0$, the Hubbard model has an insulating ground state at half-filling. The insulating state is a Mott insulator with a Mott-Hubbard gap in the density of states. Away from half-filling, the DOS of the one-dimensional system remains gapless for all values of U and the system is in a metallic state. In finite dimensions $D > 1$, no exact solution exists at the moment and only numerical results are available. However, already numerically, the exact treatment of the Hubbard model is complicated and still a non-trivial challenge. Due to limitations of computer time and memory, exact methods like numerical diagonalization and quantum Monte Carlo are restricted to rather small system sizes. However, some important features can already be understood using qualitative arguments, for example the formation of an insulating, anti-ferromagnetic ground state at half filling. For large values of U, at half-filling, charge fluctuations will be energetically unfavorable and, on average, each site will be occupied by exactly one electron. Virtual hopping processes will be allowed for electrons with opposite spins at neighboring sites. Thus, an anti-ferromagnetic ground state will be favorable. Formally, this means that the Hubbard model becomes equivalent to the Heisenberg model, i.e. the so-called $t - J$ model [132] at half-filling.

5.2.3 Combining correlation and disorder: the Anderson-Hubbard model in general

In the previous section, the Hubbard model was introduced as the minimal lattice model of strongly correlated systems. If one is interested in the interplay of disorder and interactions, one needs to treat both potentials on the same level. Therefore, it is a natural and convenient choice to combine the Hubbard model with disordered

single-particle Anderson model to obtain an interacting, disordered many-body system [133]. The applicability of the Anderson-Hubbard model to real materials is not very clear. The Hubbard model was originally motivated by the assumption of a strong screening of the bare Coulomb interaction. Therefore the effective interaction was reduced to a purely local one. However, the effective range of the Coulomb interaction in disordered materials might be significantly larger since localized electrons are much less mobile than the conduction electrons.

However, the Anderson-Hubbard model, as the simplest non-trivial lattice model for interacting particles in a disordered environment, is a good starting point in understanding of strongly interacting, disordered systems. And it is already the source of rather rich and complex physics. It should also be mentioned that, in the recent years, the field of cold atomic gases in optical potentials has established itself as a new area of research with close connections to condensed matter theory [134]. While results from the Anderson-Hubbard model can only give a qualitative description of the physical processes of real materials, the Anderson-Hubbard model can provide a very good description of many experiments in cold atomic gases.

In summary, no rigorous statements, and almost no generally accepted, conclusive analytic results on the problem of Anderson localization in interacting systems have been presented yet. Much effort has been made via numerical studies to get a deeper insight into the problem. But also for numerical studies, many contradictory results have been obtained, and many issues remain open.

5.2.4 Combining correlation and disorder: the Anderson-Hubbard model in quantum transport

In this thesis, we investigate short interacting and disordered chains attached to homogeneous contacts. The chains are described by a finite-size realization of the Anderson-Hubbard model. In standard notation, taking into account a possible time dependence (τ is the time variable), the lattice system we consider in a quantum transport setup is described by the following Hamiltonian:

$$H = \sum_{\sigma} \sum_{l=-\infty}^{\infty} V_{l,l+1}(a_{l\sigma}^{\dagger} a_{l+1,\sigma} + H.c.) + \sum_{\sigma} \sum_{l=1}^{L} \left[\epsilon_l + \frac{U}{2} \hat{n}_{l-\sigma} \right] \hat{n}_{l\sigma} + b_S(\tau) \sum_{l<1,\sigma} \hat{n}_{l.\sigma} + b_D(\tau) \sum_{l>L,\sigma} \hat{n}_{l.\sigma}. \qquad (5.34)$$

Eq.(5.34) describes a central chain of length L (the lattice sites with $1 \leq l \leq L$) connected to a left and a right 1D, homogeneous and noninteracting lead [sites with $l < 1$ and $l > L$, respectively]. The third and fourth terms of Eq. (5.34) represent the time-dependent bias in the leads which is applied at time $\tau \geq 0$. This term is

necessary to induce currents in the system. The hopping term $V_{l,l+1} = -1$ always, i.e. we employ transparent boundary conditions.

We consider diagonal uniform disorder, i.e. $\epsilon_l \in [-W/2, W/2]$, but in Paper IV we will sometimes introduce binary disorder, where $\epsilon_l = \pm W/2$. In both cases, W fixes the strength of the disorder. We limit ourselves to the case of a repulsive interaction, i.e. $U > 0$ always.

To characterize the degree of localization, we use the inverse participation ratio (IPR). The IPR of Eq.(5.32) can be modified in the following two possible ways to deal with interacting systems:

$$\zeta_1 = \sum_i^M \Delta n_i^2 / (\sum_i^M \Delta n_i)^2, \tag{5.35}$$

$$\zeta_2(\omega) = \sum_i^M n_i^2(\omega) / [\sum_i^M n_i(\omega)]^2. \tag{5.36}$$

The use of ζ_1 is convenient when dealing with small systems with discrete many-body levels [135]. In this case, for N particles, Δn_i is the difference between the ground-state densities with $N+1$ and N particles, a clear operational prescription for finite systems. Using ζ_2 [136] amounts to consider the density of states as obtained from the one-particle propagator, since $n_i(\omega) = -\Im G_{ii}(\omega)/\pi$. It should be noted that most investigations of IPR are done numerically, for finite systems. Using ζ_2 requires introducing a finite artificial broadening, and employing a finite-size scaling analysis, to assess the role of γ [137, 138, 139]. To deal with infinite systems, as those of Eq. (5.34), a further modification to the IPR is required. This is discussed in Paper IV.

5.2.5 Lattice (TD)DFT and its use in quantum transport

The lattice version of DFT relies on the fact that there is a one-to-one correspondence between local potentials v_i and the ground-state expectation values of the site occupations n_i [140]. Therefore it is in principle possible to express all quantities that can be obtained from the ground-state wave function as a function of the densities. The site occupations as a function of the potentials can be found from derivatives of the ground-state energy with respect to the local potential.

A DFT formulation based on the local lattice occupation numbers n_i was introduced more than two decades ago, to describe some ground state properties of the Hubbard model [141, 142, 143]. Further significant progress came with a local-density approximation (LDA) for the inhomogeneous 1D Hubbard model [140] (based on the Bethe-Ansatz solution of the 1D Hubbard model and henceforth denoted BALDA). The BALDA was then used to obtain a simple analytical parameterization of the XC energy E_{xc} and potential v_{xc} [144]. In subsequent work, the BALDA was scrutinized against exact results [144, 145, 146, 147, 148],

providing energies, particle densities and entropies with an accuracy within a few percents.

The extension of lattice DFT to the time dependent case, i.e. to describe the real-time dynamics of lattice models out of equilibrium, was first proposed in Ref. [149]. We wish however to emphasize that while lattice DFT is a rigorous framework, there is at present no Runge-Gross (RG) theorem directly for lattice TDDFT, as discussed in Ref. [150]. On the other hand, with the bond-current as the basic variable, a rigorous formulation of time-dependent current-density-functional theory on the lattice becomes possible [151, 152, 150]. Finally, it should also be noted that in 1D systems, there is a one-to-one correspondence between densities and currents, and thus TDDFT as proposed in [149] already rests on solid grounds.

In this work, we confine ourselves to the non magnetic 1D case and we describe here the actual formulation for spin-independent (TD)DFT. In standard DFT notation, we can write for the ground-state total energy [143, 140]:

$$E[n, v_{ext}] \equiv T_0[n] + E_H[n] + E_{xc}[n] + \sum_i v_{ext}(i) n_i, \tag{5.37}$$

where $v_{ext}(i) \equiv \epsilon_i$ is the static external field, $T_0[n]$ the non-interacting kinetic energy and E_H the Hartree energy, with $n_i = \sum_\sigma n_{i\sigma}$. To perform a local density approximation, E_{xc} is obtained from a homogeneous reference system, i.e. the 1D Hubbard model:

$$E_{xc} = E - T_0 - E_H \ . \tag{5.38}$$

To obtain v_{xc}, one takes the derivative of the XC energy per site $e_{xc} \equiv E_{xc}/L$ with respect to the density (in the general case, this should be a functional derivative):

$$v_{xc} = \frac{\partial e_{xc}(n, U)}{\partial n} \ . \tag{5.39}$$

For bipartite lattices, $e_{xc}(n, U) = e_{xc}(2 - n, U)$ in the entire density range $[0, 2]$ and thus $v_{xc}(n) = -v_{xc}(2 - n)$. The Hartree potential is written as

$$v_H(i) = \frac{\delta E_H}{\delta n_i} = \frac{\delta}{\delta n_i} \frac{1}{4} \sum_j U_j n_j^2 = \frac{1}{2} U_i n_i \tag{5.40}$$

The ground state energy can be calculated once the ground state is known, using (see [145])

$$E = \sum_i^N e_i - V_H[n] + E_{xc}[n] - \int n(r) \frac{\delta E_{xc}[n]}{\delta n} d\mathbf{r} \tag{5.41}$$

where the first term is the sum of the Kohn-Sham eigenvalues, the second term is the contribution from the Hartree term, the third term is the exchange energy term, and finally the last term is from the exchange-correlation potential. Finally, a local-density approximation (LDA) is defined:

$$v_{xc}(i) = v_{xc}^{BALDA}(n_i). \tag{5.42}$$

In ground-state DFT-LDA calculations, the XC potential obtained in this way is used to solve self-consistently the Kohn-Sham (KS) equations

$$(\hat{t} + \hat{v}_{KS})\varphi_\kappa = e_\kappa \varphi_\kappa \quad , \tag{5.43}$$

where $\hat{t}$ denotes the matrix for the single-particle hoppings between nearest - neighboring sites, and φ_κ is the $\kappa - th$ single-particle KS orbital, with $n_i = \sum_\kappa^{occ} |\varphi_\kappa(i)|^2$. The effective potential matrix is diagonal:

$$(\hat{v}_{KS})_{ii} = v_{KS}(i) = v_H(i) + v_{xc}(i) + v_{ext}(i) \tag{5.44}$$

with $v_H(i) = \frac{1}{2} U_i n_i$ being the Hartree potential. In analogy with the continuum case, the lattice Kohn-Sham (KS) equations can be propagated in time, to get a TDDFT description of the dynamics of lattice systems [149]. For this, one needs to solve the time-dependent KS equations on the lattice,

$$i\partial_\tau \varphi_\kappa(\tau) = \left(\hat{t} + \hat{v}_{KS}(\tau)\right) \varphi_\kappa(\tau) \tag{5.45}$$

$$v_{KS}(i,\tau) = v_H(i,\tau) + v_{xc}(i,\tau) + v_{ext}(i,\tau). \tag{5.46}$$

In general $v_{xc}(i,\tau)$, depends non-locally in space and time on the density. In the adiabatic local density approximation (ALDA) [153] to the XC potential,

$$v_{xc}^{ALDA}(i,\tau) \equiv v_{xc}^{BALDA}(n_i(\tau)) \tag{5.47}$$

$$n_i(\tau) = \sum_\kappa^{occ} |\varphi_\kappa(i,\tau)|^2. \tag{5.48}$$

An ALDA for the Hubbard model, denoted in the literature as ABALDA, was first introduced In Ref. [149], with the treatment was limited to spin-compensated systems, while the spin-dependent case was presented in Ref. [154], where TDDFT results and time-dependent DMRG results were compared.

For finite systems, a comparative study more focused on the role of non-local and memory effects beyond the ALDA was performed in Ref. [155], comparing the ALDA, exact, and Kadanoff-Baym time-evolution in small cubic Hubbard clusters. The KBE, with a many-body perturbation-theory approach to the self-energy, permit to take into account non-locality and memory effects on equal footing. Such comparisons showed that an ALDA coming from the appropriate (strongly correlated) reference system can perform well in many instances, (especially for

slow perturbations) but, quite generally, it will fail for fast perturbations, or very strong interactions.

In a TDDFT approach to time-dependent quantum transport [107, 108], a central ingredient is the XC potential. According to Eq.(5.38), to construct an LDA in 1D we need the exact ground-state energy of the infinite homogeneous 1D Hubbard model, where the hopping $V_{l,l+1} \equiv V$ and the interaction is present at all sites. In the most general case, e.g. in the presence of magnetic effects, this requires [144, 147, 156] to solve the coupled Bethe-Ansatz equations for the charge and spin distribution functions [$\rho(x)$ and $\sigma(x)$, respectively] [131]. An ALDA is then easily obtained [149, 154], making v_{xc} to become a function of the instantaneous local density. In this thesis we confine ourselves to the non-magnetic case (where the spin-up and spin-down densities are equal, i.e. $n_\uparrow = n_\downarrow = n/2$). The XC potential is discontinuous at half-filling; however, for a finite interacting system contacted to non-interacting leads, the discontinuity of the exact v_{xc} becomes slightly smoothed (this was already pointed out in Ref. [157], using support from small Anderson clusters, and fully discussed in Refs. [158, 159, 160]). According to these considerations, and also for numerical convenience, the XC potential was slightly smoothed in our actual calculations.

The open-boundary scheme for quantum transport used in this work is the one developed in Ref. [109], while similarly to Ref. [157], interactions in the central region are treated via the adiabatic local density approximation from the Bethe Ansatz [149]. However, for disordered systems, where large central regions and configuration averages may be needed, such algorithm may result computationally expensive. A way to enhance the numerical efficiency of such algorithm using the Lanczos recursion technique was preliminarily discussed in Ref. [161] and is presented in detail in Paper IV.

Bibliography

[1] P. T. Lang, F. Sessler, U. Werling, and K. F. Renk, Appl. Phys. Lett. **55**, 2576 (1989).

[2] E.F. Venger, S.G. Gasan-zade, M.V. Strikha, S.V. Stary, G.A. Shepel'ski, Semiconductors, vol. 34, pp. 763-767, 2000.

[3] Special Issue on Far-infrared Semiconductor Lasers. Eds: E. Gornik, A.A Andronov, Optical and Quantum Electronics, vol. 23, Issue 2, pp. S111-S349, 1991.

[4] Iotti R. C. and Rossi F. 2001 Phys. Rev. Lett. 87 146603; Köhler R, Iotti R. C., Tredicucci A. and Rossi F. 2001 Appl. Phys. Lett. 79 3920(R); Köhler, A. Tredicucci, F. Beltram, H. E. Beere, E. H. Linfield, A. G. Davies, D. A. Ritchie, R. C. Iotti3 and F. Rossi 2002 Nature 417 156

[5] K. Donovan, P. Harrison, and R. W. Kelsall, J. Appl. Phys. 89, 3084 (2001). K. Kalna, C. Y. L. Cheung, and K. A. Shore, J. Appl. Phys. 89, 2001 (2001). D. Indjin, P. Harrison, R. W. Kelsall, and Z. Ikonic, IEEE Photonics Technol. Lett. 15, 15 (2003).

[6] S. Barbieri, F. Beltram, and F. Rossi, Phys. Rev. B 60, 1953 (1999).

[7] C. Jacoboni and L. Reggiani, Rev. Mod. Phys. **55**, 645 (1983).

[8] A. Cho, Molecular Beam Epitaxy (AIP Press, Woodbury, New York, 1994).

[9] T. Ando, A. B. Fowler, and F. Stern, Rev. Mod. Phys. 54, 437 (1982).

[10] G. Bastard and J. P. Brum, IEEE J. Quantum Electron. QE-22, 1625 (1986).

[11] David K. Ferry, Stephen M. Goodnick *Transport in nanostructures* (Cambridge university press, 1997)

[12] L. Esaki and R. Tsu, IBM J. Res. Dev. 14, 61 (1970).

[13] F. Bloch, Z. Phys. 52 (1928) 555.

[14] G.H. Wannier, Phys. Rev.117 (1960) 432.

[15] Kuijuan Jin, M. Odnoblyudov, Y. Shimada, K. Hirakawa, and K. A. Chao, Phys. Rev. B 68, 153315 (2003).

[16] G. H. Wannier, Rev. Mod. Phys. 34, 645 (1962).

[17] N. Sekine and K. Hirakawa, Phys. Rev. Lett. 94, 057408 (2005).

[18] E. M. Lifshitz and L. P. Pitaevskii, Physical Kinetics (Pergamon, New York, 1981)

[19] P. Y. Yu and M. Cardona, *Fundamentals of Semiconductors*, 2nd ed. (Springer Verlag, Berlin, 1999).

[20] C. Moglestue, *Monte Carlo Simulation of Semiconductor Devices* (Chapman & Hall, London, 1993).

[21] T. Kurosawa, in Proc., Int. Conf.Phys. Semiconductors, Kyoto (1966) J. Phys. Soc.Japan Suppl. 24, 424-6 .

[22] P. J. Price, IBM J. Res. Dev. 17, 39 (1973).

[23] H. D. Rees, Phys. Lett. **A26**, 416 (1968); J. Phys. Chem. Solids **30**, 643 (1969).

[24] W. Fawcett, H. D. Rees, Phys. Lett. 11, 731 (1969).

[25] W. Fawcett, C. Hilsum, and H. D. Rees, Solid State Commun. **7**, 1257 (1969).

[26] W. Fawcett, A. D. Boardman and S. Swain, J. Phys. Chem. Solids **31**, 1963 (1970).

[27] W. Fawcett, *Electrons in Crystalline Solids*, edited by A. Salam (IAEA, Vienna, 1973), p. 531.

[28] P. A. Lebwohl and P. J. Price, Solid State Commun. **9**, 1221 (1971).

[29] S. Bosi, C. Jacoboni, J. Phys. C9, 315 (1976).

[30] P. Lugli and D. K. Ferry, IEEE Trans. Electron Devices **ED-32**, 2431 (1985).

[31] C. Jacoboni and P. Lugli, The Monte Carlo Method for Semiconductor Device Simulation (Springer, Vienna, 1989).

[32] U. Fano, Phys. Rev. **124**, 1866 (1961).

[33] R. Buczko and F. Bassani, Phys. Rev. B **45**, 5838 (1992).

[34] A. Onton, P. Fisher, and A.K. Ramdas, Phys. Rev. **163**, 686 (1967).

[35] A. Onton, Phys. Rev. B **4**, 4449 (1971).

[36] E. Goldys, P. Galtier, G. Martinez, and I. Gorczyca, Phys. Rev. B **36**, 9662 (1987).

[37] M. A. Odnoblyudov, I. N. Yassievich, V. M. Chistyakov, M. S. Kagan, and K.-A. Chao, Phys. Rev. **B62**, 2486 (2000).

[38] F. Capasso, C. Sirtori, J. Faist, D.L. Sivco, S.-N.G. Chu, and A.Y. Cho, Nature (London) **358**, 565 (1992).

[39] C. Sirtori, F. Capasso, J. Faist, and S. Scandolo, Phys. Rev. B **50**, 8663 (1994).

[40] D.Y. Oberli, G. Böhm, G. Weimann, and J.A. Brum, Phys. Rev. B **49**, 5757 (1994).

[41] S. Glutsch, D.S. Chemla, and F. Bechstedt, Phys. Rev. B **51**, 16 885 (1995).

[42] S. A. Lynch, S. S. Dhillon, R. Bates, D. J. Paul, D. D. Arnone, D. J. Robbins, Z. Ikonic, R. W. Kelsall, P. Harrison, D. J. Norris, A. G. Cullis, C. R. Pidgeon, P. Murzyn, and A. Loudon, Mater. Sci. Eng., B **89**, 10 (2002).

[43] I.V. Altukhov, E.G. Chirkova, V.P. Sinis, M.S. Kagan, Y.P. Gousev, S.G. Thomas, K.L. Wang, M.A. Odnoblyudov, and I.N. Yassievich, Appl. Phys. Lett. **79**, 3909 (2001).

[44] A. Blom, M.A. Odnoblyudov, H.H. Cheng, I.N. Yassievich, and K.A. Chao, Appl. Phys. Lett. **79**, 713 (2001).

[45] G. Masini, L. Colace, and G. Assanto, Mater. Sci. Eng., B **89**, 2 (2002).

[46] D.D. Arnone, C.M. Ciesla, and M. Pepper, Phys. World **13** (4), 35 (2000).

[47] R.L. Greene and K.K. Bajaj, Phys. Rev. B **31**, 4006 (1985).

[48] S. Fraizzoli, F. Bassani, and R. Buczko, Phys. Rev. B **41**, 5096 (1990).

[49] A. Blom, M. A. Odnoblyudov, I. N. Yassievich, and K.-A. Chao, Phys. Rev. **B65**, 155302 (2002).

[50] K. Jayakumar, S. Balasubramanian, and M. Tomak, Phys. Rev. B **34**, 8794 (1986).

[51] C. Priester, G. Allan, and M. Lannoo, Phys. Rev. B **29**, 3408 (1984).

[52] S.T. Yen, Phys. Rev. B **66**, 075340 (2002).

[53] A. Blom, M.A. Odnoblyudov, I.N. Yassievich, and K.A. Chao, Phys. Status Solidi B **235**, 85 (2003).

[54] A.A. Prokofev, I.N. Yassievich, A. Blom, M.A. Odnoblyudov, and K.A. Chao, Nanotechnology **12**, 457 (2001).

[55] T.A. Perry, R. Merlin, B.V. Shanabrook, and J. Comas, Phys. Rev. Lett. **54**, 2623 (1985).

[56] M. Helm, F.M. Peeters, F. DeRosa, E. Colas, J.P. Harbison, and L.T. Florez, Phys. Rev. B **43**, 13 983 (1991).

[57] A. Sibille, J. F. Palmier, C. Minot, and F. Mollot, Appl. Phys. Lett. **54**, 165 (1989).

[58] J. Feldmann, K. Leo, J. Shah, D. A. B. Miller, J. E. Cunningham, T. Meier, G. von Plessen, A. Schulze, P. Thomas, and S. Schmitt-Rink, Phys. Rev. B 46, R7252 (1992).

[59] K. Leo, P. Haring Bolivar, F. Brüggemann, R. Schwedler, and K. Köhler, Solid State Commun. **84**, 943 (1992).

[60] M. Helm, Semicond. Sci. Technol. **10**, 557 (1995).

[61] C. Waschke, H. G. Roskos, R. Schwedler, K. Leo, H. Kurz, and K. Köhler, Phys. Rev. Lett. 70, 3319 (1993).

[62] T. Dekorsy, P. Leisching, K. Köhler, and H. Kurz, Phys. Rev. B 50, R8106 (1994).

[63] K. Unterrainer, B. J. Keay, M. C. Wanke, S. J. Allen, D. Leonard, G. Medeiros-Ribeiro, U. Bhattacharya, and M. J. W. Rodwell, Phys. Rev. Lett. **76**, 2973 (1996).

[64] E. Schomburg, T. Blomeier, K. Hofbeck, J. Grenzer, S. Brandl, I. Lingott, A. A. Ignatov, K. F. Renk, D. G. Pavelíev, Y. Koschurinov, B. Y. Melzer V. M. Ustinov, S. V. Ivanov, A. Zhukov, and P. S. Kopíev, Phys. Rev. B **58**, 4035 (1998).

[65] R. F. Kazarinov and R. A. Suris, Sov. Phys. Semicond. **6**, 120 (1972).

[66] S. A. Ktitorov, G. S. Simin, and V. Y. Sindalovskii, Fiz. Tverd. Tela (Leningrad) 13, 2230 (1971) Sov. Phys. Solid State 13, 1872 (1971)

[67] X. L. Lei, N. J. M. Horing, and H. L. Cui, Phys. Rev. Lett. **66**, 3277 1991

[68] A. A. Ignatov, K. F. Renk, and E. P. Dodin, Phys. Rev. Lett. 70, 1996 (1993).

[69] A. Wacker, G. Schwarz, F. Prengel, and E. Schöll, Phys. Rev. B **52**, 13788 (1995).

[70] F. Löser, Yu. A. Kosevich, K. Köhler, and K. Leo , Phys. Rev. B 61, R13373 (2000).

[71] Y. Shimada, K. Hirakawa, and S.-W. Lee, Appl. Phys. Lett. 81, 1642 (2002).

[72] G. Bastard and R. Ferreira, C. R. Acad. Sci., Ser. II: Mec., Phys., Chim., Sci. Terre Univers 312, 971 (1991).

[73] A. Wacker, Phys. Rev. B 66,085326 (2002).

[74] R. Tsu and G. Döhler, Phys. Rev. B 12, 680 (1975).

[75] M. A. Odnoblyudov, I. N. Yassievich, M. S. Kagan, Yu. M. Galperin, and K. A. Chao, Phys. Rev. Lett. 83, 644 (1999).

[76] I. V. Altukhov, E. G. Chirikova, M. S. Kagan, K. A. Korolev, V. P. Sinis, and F. A. Smirnov, Sov. Phys. JETP 74, 404 (1992).

[77] A. Blom, M. A. Odnoblyudov, I. N. Yassievich, and K.-A. Chao, Phys. Rev. **B68**, 165338 (2003).

[78] M. M. Rieger and P. Vogl, Phys. Rev. B **48**, 14276 (1993).

[79] H. Yaguchi, K. Tai, K. Takemasa, K. Onabe, R. Ito, and Y. Shiraki, Phys. Rev. **B49**, 7394 (1994).

[80] B. K. Ridley, *Quantum processes in semiconductors*, 2nd ed. (Clarendon Press, Oxford, 1988).

[81] D. K. Ferry, Phys. Rev. **B14**, 1605 (1976).

[82] C. Canali, C. Jacoboni, F. Nava, G. Ottaviani, and A. Alberigi-Quaranta, Phys. Rev. **B12**, 2265 (1975).

[83] P. Dollfus, J. Appl. Phys. **82**, 3911 (1997).

[84] H. Miyata, T. Yamada, and D. K. Ferry, Appl. Phys. Lett. **62**, 2661 (1993).

[85] P. K. Basu and S. K. Paul, J. Appl. Phys. **71**, 3617 (1992).

[86] F. Löser, Yu. A. Kosevich, K. Këhler, and K. Leo, Phys. Rev. B 61, R13373 (2000).

[87] L. K. Orlov and Yu. A. Romanov, Fiz. Tverd. Tela (Leningrad) 19, 726 (1977) Sov. Phys. Solid State 19, 421 (1977)

[88] Yu. A. Romanov, V. Bovin, and L. Orlov, Fiz. Tekh. Poluprovodn. (S.-Peterburg) 12, 1665 (1978) Sov. Phys. Semicond. 12, 987 (1978)

[89] L. W. Wang, A. Zunger, and K. A. Mader, Phys. Rev. B 53, 2010 (1996).21P. Ray and P. K. Basu, Phys. Rev. B 45, 9169 (1992).

[90] G. Cuniberti, *Introducing Molecular Electronics* (Publisher Springer Berlin/Heidelberg, 2005),

[91] N. D. Lang, Phys. Rev. B **52**, 5335 (1995).

[92] N. D. Lang and P. Avouris, Phys. Rev. Lett. **81**, 3515 (1998).

[93] M. Di Ventra, S. T. Pantelides1, and N. D. Lang , Phys. Rev. Lett. **84**, 979 (2000)

[94] Mads Brandbyge1, José-Luis Mozos, Pablo Ordejón, Jeremy Taylor, and Kurt Stokbro, Phys. Rev. B 65 **16**, 165401 (2002)

[95] F. Evers, F. Weigend, and M. Koentopp, Phys. Rev. B **69**, 235411 (2004)

[96] Max Koentopp, Connie Chang, Kieron Burke and Roberto Car, J. Phys.: Condens. Matter **20** 083203 (2008)

[97] L. P. Kadanoff and G. Baym, *Quantum Statistical Mechanics* (W. A. Benjamin, Inc. New York, 1962).

[98] L. V. Keldysh, JETP **20**, 1018 (1965).

[99] N. Bushong, Y. Pershin, and M. Di Ventra, Phys. Rev. Lett. **99**, 226802 (2007)

[100] N. Sai, N. Bushong, R. Hatcher, and M. Di Ventra, Phys. Rev. B **75**, 115410 (2007)

[101] J. Yao, Y.-C. Chen, M. Di Ventra, and Z. Q. Yang, Phys. Rev. B **73**, 233407 (2006)

[102] J. S. Evans, C. L. Cheng, T. Van Voorhis, Phys. Rev. B **78**, 165108 (2008).

[103] J. S. Evans and T. Van Voorhis, Nano. Lett. **9**, 2671 (2009).

[104] J. S. Evans, O. A. Vydrov, T. Van Voorhis, J. Chem. Phys. **131**, 034106 (2009).

[105] C. Chien, M. Zwolak, M. Di Ventra, Phys. Rev. A **85**, 041601 (2012)

[106] M. Cini, Phys. Rev. B **22**, 5887 (1980).

[107] G. Stefanucci and C.-O. Almbladh, Phys. Rev. B **69**, 195318 (2004).

[108] G. Stefanucci and C.-O. Almbladh, EPL **67**, 14 (2004).

[109] S. Kurth, G. Stefanucci, C.-O. Almbladh, A. Rubio, E. K. U. Gross, Phys. ReV. B **72**, 035308 (2005)

[110] P. Myöhänen, A. Stan, G. Stefanucci, R. van Leeuwen, EPL **84**, 67001 (2008).

[111] Petri Myöhänen, Adrian Stan, Gianluca Stefanucci, and Robert van Leeuwen, Phys. Rev. B **80**, 115107 (2009).

[112] M. Puig von Friesen, C. Verdozzi, and C.-O. Almbladh, J. Phys.: Conf. Ser. 220 012016 (2010)

[113] C. Verdozzi, G. Stefanucci, C.-O. Almbladh, Phys. Rev. Lett. **97**, 046603 (2006).

[114] P. Hohenberg and W. Kohn, Phys. Rev., **136**:B864, 1964

[115] W. Kohn and L.J. Sham. Phys. Rev., 140:A1133, 1965
L.J. Sham and Walter Kohn. Phys. Rev., 145:561, 1966.

[116] M. Levy, Proceedings of the National Academy of Sciences **76** 6072 (1979)

[117] C.-O. Almbladh and U. von Barth, Phys. Rev. B **31**, 3231 (1985).

[118] Ulf von Barth. Many-Body Phenomena at Surfaces. Academic Press, New York, 1984.

[119] E. Runge and E. K. U. Gross. Phys. Rev. Lett., **52**:997, 1984.

[120] P. W. Anderson, Phys. Rev. **109**, 1492 (1958).

[121] F. J. Wegner, Z. Phys B **25** 327 (1976)

[122] E. Abrahams, P. W. Anderson, D. C. Licciardello T. V. Ramakrishnan, Phys. Rev. Lett. **42**, 673 (1979).

[123] N. F. Mott and W. D. Twose, Adv. Phys. **10**, 107 (1961).

[124] T. N. Zavaritskaya and E. I. Zavaritskaya, JETP Lett. **45**, 609 (1987).

[125] S. V. Kravchenko, G. V. Kravchenko, J. E. Furneaux, V. M. Pudalov and M. D'Iorio, Phys. Rev. B **50**, 8039 (1994).

[126] S. V. Kravchenko, W. E. Mason, G. E. Bowker, J. E. Furneaux, V. M. Pudalov and M. D'Iorio, Phys. Rev. B **51**, 7038 (1995).

[127] S. V. Kravchenko, D. Simonian, M. P. Sarachik, W. Mason and J. E. Furneaux, Phys. Rev. Lett. **77**, 4938 (1996).

[128] D. Popovíc, A. B. Fowler and S. Washburn, Phys. Rev. Lett. **79** 1543 (1997).

[129] J. Hubbard, Proc. Roy. Soc. A **276**, 238 (1963).

[130] E. H. Lieb, in Proceedings of the XI International Congress of Math- ematical Physics, edited by D. Iagolnitzer (Int. Press Inc., Boston, 1995), p. 392.

[131] E.H. Lieb and F.Y. Wu, Phys. Rev. Lett. **20**, 1445 (1968).

[132] K. A. Chao, J. Spalek, A. M. Oles, J. Phys. C **10**, L271 (1977).

[133] M. Ma, Phys. Rev. B **26**, 5097 (1982).

[134] D. Jaksch, P. Zoller, Ann. Phys. **315**, 52 (2005).

[135] B. Srinivasan, G. Benenti, D. L. Shepelyanski, Phys. Rev. B **67**, 205112 (2003).

[136] Y. Song, R. Wortis, and W. A. Atkinson, Phys. Rev. B **77**, 054202 (2008).

[137] G. Schubert, J. Schleede, K. Byczuk, H. Fehske, D. Vollhardt, Phys. Rev. B **81**, 155106 (2010).

[138] N. C. Murphy, R. Wortis, and W. A. Atkinson, Phys. Rev. B **83**, 184206 (2011).

[139] S. Johri and R. N. Bhatt, arXiv:1106.1131v2.

[140] K. Schönhammer, O. Gunnarsson, R.M. Noack, Phys. Rev. B**52**, 2504 (1995).

[141] O. Gunnarsson and K. Schönhammer, Phys. Rev. Lett. **56** (1986).

[142] K. Schönhammer, O. Gunnarsson, J. Phys. C: Solid State Phys. **20**, 3675 (1987).

[143] K. Schönhammer, O. Gunnarsson, Phys. Rev. B **37**, 3128 (1988).

[144] N. A. Lima, M. F. Silva, and L. N. Oliveira, Phys. Rev. Lett. **90** 146402 (2003).

[145] N.A. Lima, L.N. Oliveira, and K. Capelle, Europhys. Lett. **60**, 601 (2002).

[146] M.F. Silva, N.A. Lima, A.L. Malvezzi, and K. Capelle, Phys. Rev. B **71**, 125130 (2005).

[147] G. Xianlong, M. Polini, M.P. Tosi, V.L. Campo, K. Capelle, and M. Rigol, Phys. Rev. B **73**, 165120 (2006).

[148] V. V. França and K. Capelle, Phys. Rev. A **74**, 042325 (2006); Phys. Rev. Lett. **100**, 070403 (2008).

[149] C. Verdozzi, Phys. Rev. Lett. **101**, 166401 (2008).

[150] S. Kurth and G. Stefanucci, Chemical Physics **391**, 164 (2011).

[151] G. Stefanucci, E. Perfetto, and M. Cini, Phys. Rev. B **81**, 115446 (2010).

[152] I. Tokatly, Phys. Rev. B **83**, 035127 (2011).

[153] A. Zangwill and P. Soven, Phys. Rev. A **21**, 1561 (1980).

[154] Wei Li, Gao Xianlong1, Corinna Kollath, and Marco Polini, Phys. Rev. B **78**, 195109 (2008).

[155] C. Verdozzi, D. Karlsson, M. Puig von Friesen, C.-O. Almbladh, U. von Barth, Chemical Physics **391**, 37 (2011).

[156] A. Akande, S. Sanvito, Phys. Rev. B **82**, 245114 (2010).

[157] S. Kurth, G. Stefanucci, E. Khosravi, C. Verdozzi, and E. K. U. Gross, Phys. Rev. Lett. **104**, 236801 (2010).

[158] J. P. Bergfield, Z. -f. Liu, K. Burke and C. A. Stafford, Phys. Rev. Lett. **108**, 066801 (2012).

[159] G. Stefanucci and S. Kurth, Phys. Rev. Lett. **107**, 216401 (2011).

[160] P. Tröster, P. Schmitteckert, F. Evers, Phys. Rev. B. **85**, 115409 (2012).

[161] An early discussion of the modified algorithm can be found in C. Verdozzi, C.-O. Almbladh, arXiv:0808.1643.

Chapter 6

Brief summaries of the papers

Paper I

We present Monte Carlo simulations of the kinetic properties of various two-dimensional semiconductor hetero-structures. The main idea is to investigate the influence of different scattering mechanisms on the kinetic properties, for those particular systems which require accurately calculated scattering probabilities. The model we developed was applied to two distinct hetero-structures.

Paper II

We performed Monte Carlo simulations of the electron drift velocity in a δ-doped Si/SiGe quantum well, for high and low temperatures as well as strong and weak electric fields, which were applied parallel to the quantum well layer. We gave the analytical expressions of all relevant scattering probabilities and used them to calculate the distribution function. All scattering matrix elements of inter-valley phonons, acoustic phonons, interface roughness, and impurity ions were calculated from the electron wave functions. In terms of the numerical results obtained with such approach, we discussed the importance of each scattering mechanism in various ranges of temperature and the strength of electric field applied parallel to interfaces. Special attention was paid to the resonant state scattering which, at the time of our work, was far from being understood, both theoretically and experimentally. Our results show for the first time the dramatic effect of the resonant-state scattering on the electron drift velocity. The relative relaxation times of various scattering mechanisms are also derived from the Monte Carlo simulations.

Paper III

We have modified the Monte Carlo technique developed in Paper I and II in order to take into account the electron transport between quantum well layers induced by electric fields applied along the growth direction. This has made possible to investigate the mechanism of scattering-assisted charge transport in semiconductor superlattices under a strong applied electric field in the Wannier-Stark (WS) regime. The distribution function of quasi-two-dimensional carriers localized in each WS level has been calculated, and the contributions of different scattering mechanisms to the total scattering probability have been analyzed. Based on these results, the drift velocity was derived as a function of the applied electric field. Our simulated I-V characteristics oscillate with clear negative differential velocity behaviour. We show that such a dependence is determined by LO-phonon-induced resonant transfer of electrons between different spatially localized Wannier-Stark states. Our theoretical results agree with the experimental data which were obtained from analyzing the terahertz response of superlattices to picosecond optical pulse excitations.

- For the projects presented in Papers I-III, I developed the code necessary to perform all the simulations in Paper I and II. The code is based on the Monte Carlo method and gives distribution functions and other kinetic parameters within a quantum well geometry. In Paper III, the main object of interest was transport in superlattices, i.e. transitions between different quantum structures. Thus, my code had to be generalized to take this into account. This development was done by me and Yuriy Tarakanov, and our contributions are in my judgement about equal. I performed most of the calculations used in the three papers and actively participated in theoretical development and other scientific discussions. In quality of first author in Papers I and II, I wrote the first draft of these papers.

Paper IV

The static and dynamical behaviour of 1D systems are investigated. The focus is on how the interplay of interactions and disorder affects the localization of fermions in Hubbard chains, contacted to semi-infinite leads. The main tool was (TD)DFT in its lattice formulation. The localization of the electrons is characterized via the inverse participation ratio, for both the static and time-dependent cases. The transport properties of our quantum system were obtained via real-time propagation of wave functions within TDDFT. A well known embedding technique was used to properly take into account the presence of semi-infinite leads. To increase its efficiency we modified it via the recursive Lanczos method. We find a dynamical enhancement of delocalization in presence of a finite bias, and an increase of

the steady-state value of the current, induced by inter-particle interactions. For contacted chains, we analyzed the spectral properties as obtained by the coherent-potential approximation with interactions included via lattice DFT. Using short isolated chains with interaction and disorder, a brief comparative analysis between lattice (TD)DFT and exact results was also made.

- In this project, most results were produced with a previously developed (TD)DFT code which I modified to deal with the case of disordered systems. I also introduced modifications in an exact-diagonalization code, to use it in the case of disordered clusters. I performed all the actual calculations, and a preliminary analysis of all data. I was actively involved in all the scientific discussions, and in the writing of the paper.